



Camille Duclos

Nanotech 2024/2025 ONERA

29 Av. de la Division Leclerc, 92320 Chatillon

Development and characterization of MEMS vibrating gyroscope electronics

From 17/02/2025 to 18/07/2025

Under the supervision of:

- Company Supervisor: Jean GUERARD, jean.guerard@onera.fr
- Phelma Tutor: Liliana, PREJBEANU, liliana.buda@cea.fr

Confidentiality : □ yes **no**

Ecole nationale supérieure de physique, électronique, matériaux

Phelma

Bât. Grenoble INP - Minatec 3 Parvis Louis Néel - CS 50257 F-38016 Grenoble Cedex 01

Tél +33 (0)4 56 52 91 00 Fax +33 (0)4 56 52 91 03

http://phelma.grenoble-inp.fr

Acknowledgement

I would particularly like to thank Jean, my internship supervisor, for his warm welcome, his availability, and the invaluable advice he provided me throughout this experience. His guidance allowed me to acquire new skills in instrumentation. I learned a lot from his side.

I would also like to express my gratitude to the entire CMT team for welcoming me from the moment I arrived and for the support they provided me throughout my internship.

Contents

Acknowledgement	2
List of figures	
Tables	
Acronym	
Introduction	
ONERA	
1. Presentation of gyroscopes	9
a. Optical gyroscopes: Sagnac Effect	
b. Vibrating gyroscopes: Coriolis Effect	9
2. Gytrix : A navigation grade gyroscope	10
3. Allan Variance (Characterization tool)	14
4. Nyquist Circle (Characterization tool)	17
5. North Finding Presentation	19
a. Maytagging Method	19
b. Carouseling Method	20
6. Data Simulator Presentation	22
7. North Finding Experiment	31
a. Measuring instruments: MFLI & HF2LI	31
b. VIXEN SPHINX Telescope Mount & Stepper	& CAD Part32
c. Setting up the experiment with a Python script	33
d. First measurements	35
8. Complete North Finding Experiment with the Tel	lescope Mount43
Conclusion	45
Bibliography	46
Annexes	47
Annexe A: Gantt chart	47
Annexe B : Data Processing	47
Annexe C: Scenario Description	50
Résumé	51
Abstract	51
Sommario	52
Summary Sheet	53

List of figures

Figure 1: The photo on the left represents the different ONERA centers in France and the	
photo on the right shows the Chatillon center. (Missions et Objectifs, s.d.)	8
Figure 2: Explanatory diagram of the Coriolis force.	9
Figure 3: Photos of the Gytrix gyroscope taken by the CMT team. (Thomas Perrier, 2022) 1	
Figure 4: On the left, a schematic representing the behaviour of the Gytrix gyroscope with th	
two Drive & Sense modes. On the right, a representation of Drive and Sense mode, the scale	
is in mm, showing the displacement of the Y branches	
Figure 5: Behaviour of the Drive and Sense modes when the gyroscope Gytrix is under	
rotation	11
Figure 6: Scheme showing the electronical configuration of the gyroscope to be able to read	
an angular rate.	2
Figure 7: Image of the GYTRIX gyroscope vacuum-sealed in the copper case with its	
electronic board attached to it.	13
Figure 8: Presentation of Allan Variance showing the types of noise present in a gyroscope. 1	5
Figure 9: Presentation of Allan Variance in the spectral domain showing the types of noise	
present in a gyroscope.	5
Figure 10: Allan variance of the V11 model, the red line has a slope of -1/2 representing whit	te
noise; the flat line is the one representing pink noise	
Figure 11: Two successive Nyquist circles showing the effects of unwanted couplings and the	
effects of the corrections made	8
Figure 12: Explanatory diagram of the North Finding measurement, from (Asif, 2024) 1	9
Figure 13: Explaining the Measurement Process Using the Maytagging Method2	20
Figure 14: The diagram on the left shows the path taken by the Carouseling method, which	
completes a 360° rotation at a constant speed. The diagram on the right shows what the	
gyroscope measures: a continuous sinusoidal signal of the Earth's rotational speed	21
Figure 15: The diagram on the left illustrates the path followed by the carousel method, whic	h
makes discrete measurements over 360°. The diagram on the right illustrates what the	
gyroscope measures: a sinusoidal signal reconstructed from discrete measurements of the	
Earth's rotational speed	21
Figure 16: Visualization of σmin , $\tau au1$, $\tau au2$ on the measured Allan variance done in 5 min	l
measurement2	23
Figure 17: Power spectral density of the Allan variance in the spectral domain, constructed	
from the equations above	24
Figure 18: Simulated noise from white noise	24
Figure 19: Measured noise from the V11 gyroscope	25
Figure 20: FFT of measured and simulated signals	25
Figure 21: Allan Variance of simulated and generated signals	26
Figure 22: Allan Variance of simulated (artificially modified) and generated signals	26

Figure 53: North-Finding experiment set up in the basement of an ONERA building. On the	
left, a complete view of the experiment. On the right, a zoom on the telescope mount with th	ıe
construction lines on the ground to orient the mount relative to geographic North	44
Figure 54: Gantt chart.	47
Figure 55: Display of averaged measurements of the Earth's rotation speed sorted by	
measurement orientation angle	48
Figure 56: Averaging measurements sorted by angle value.	48
Figure 57: Extraction of a cosine of amplitude 9.91°/h whose phase corresponds to the	
orientation of the local reference point relative to the North.	49
7D 1.1	
Tables	
Table 1: Types of noises in an Allan variance in time domain, with fc the high-cutoff	

Acronym

ONERA: National Office for Aerospace Studies and Research

EPIC: Public establishment of an industrial and commercial nature

MEMS: Micro Electro-Mechanical Systems

NEMS: Nano Electro-Mechanical Systems

PLL: Phase Lock Loop

PID: Proportional, Integral, Derivative Corrector

ARW: Angle Random Walk

Introduction

In a world where geolocation and navigation systems are increasingly important, the ability to accurately determine the orientation of an object or vehicle has become essential. Whether in defense, autonomous vehicles, or portable navigation devices, reliable knowledge of orientation plays a key role in overall system performance.

In this technological context, gyroscopes, and more specifically MEMS (Micro Electro-Mechanical Systems)/NEMS (Nano Electro-Mechanical Systems) gyroscopes, have established themselves as essential sensors. Compact, inexpensive, and easily integrated, these sensors can measure angular rates with good accuracy. Their use makes it possible to replace magnetic compasses in electromagnetically disturbed or confined environments, such as buildings. However, despite their many advantages, MEMS gyroscopes have certain limitations inherent to their technology, such as noise due to proximity electronics and significant sensitivity to temperature variations.

This internship addresses the challenge of improving orientation measurement, given the limitations of MEMS gyroscopes. The main objective is to set up an experiment to measure the Earth's rotational speed, also known as the North Finding Experiment. Successfully detecting this extremely weak signal (approximately a thousandth of a degree per second) is an excellent indicator of the accuracy and stability of the gyroscope used. The instrument at the heart of this experiment is the new GYTRIX (Trigonal quartz crystal gyroscope) gyroscope, whose performance must be demonstrated.

To achieve this goal, the approach implemented relies on several skills: instrumentation of the gyroscope, to create the experimental setup around the gyroscope; programming, to automate data measurement and processing via Python; and finally, signal processing, to extract and analyse relevant measurements from the observed physical phenomenon to assess the overall performance of the sensor.

This report will begin with a presentation of ONERA (National Office for Aerospace Studies and Research), where this internship took place, followed by a description of the sensor used and its technological developments, the GYTRIX. Then, the experimental implementation of the North Finding experiment will be described, showing its evolution. It will then describe the implementation of a simulator to optimize the gyroscope measurement according to its characteristics.

ONERA

ONERA is the leading French research centre in the fields of aeronautics, space and defence. Created in 1946, just after the Second World War, ONERA's initial objective was to relaunch French aeronautical research by drawing inspiration from the most advanced foreign scientific and industrial models. Since then, it has continued to play a central role in the development of key technologies for French sovereignty. (Missions et Objectifs, s.d.)

A public industrial and commercial institution under the supervision of the Ministry of the Armed Forces, ONERA employs approximately 2,000 people, who are researchers, engineers, and technicians. It is funded by both public and industrial contracts.

ONERA has multiple missions: to develop and guide research in the aerospace field; to design, build, and operate the resources necessary for this research; to disseminate results nationally and internationally and promote them to industry; to support innovation in all sectors, including those outside of aeronautics; to provide expert support to government agencies; and to contribute to research training.

ONERA is located at several sites in France, including its headquarters in Palaiseau, and in Châtillon, where the internship took place (figure 1).



 $Figure\ 1:\ The\ photo\ on\ the\ left\ represents\ the\ different\ ONERA\ centers\ in\ France\ and\ the\ photo\ on\ the\ right\ shows\ the\ Chatillon\ center.\ (Missions\ et\ Objectifs,\ s.d.)$

The DPHY is one of ONERA's major scientific entities. It brings together departments working on topics ranging from fundamental physics to applied engineering in fields. Within DPHY, the CMT (Capteurs et MicroTechnologies) team focuses its research on the design, manufacturing, and characterization of high-precision MEMS gyroscope sensors. The CMT team develops next-generation MEMS gyroscope that meet growing demands for precision.

1. Presentation of gyroscopes.

Gyroscopes are everywhere in everyday life: they are found in smartphones, drones, smartwatches, cars, and more. They measure rotational speed, which allows for several applications: detecting movement, orienting maps, and even stabilizing images.

The gyroscope is an angular rotation sensor. This device can be built on two different physical principles to measure angular velocity: the optical Sagnac effect for optical gyroscopes and the Coriolis inertia effect for vibration gyroscopes. Gyroscopes often come together with accelerometers in an IMU (Inertial Measurement Unit)

a. Optical gyroscopes: Sagnac Effect

Optical gyroscopes use the Sagnac effect, a phenomenon based on the fact that the speed of light is a constant, regardless of the reference frame. When a light beam from the same light source is sent simultaneously in two opposite directions in a loop, a rotation of the system causes a phase shift between the two beams upon arrival. This phase shift is proportional to the rotation speed, which can be measured. These optical gyroscopes are very accurate and stable over time, but they are generally very large and heavy, which makes them bulky and difficult to transport. (Sagnac Effect, s.d.)

b. Vibrating gyroscopes: Coriolis Effect

Vibrating gyroscopes use the Coriolis effect to operate. In its reference frame, when an object in linear vibration (along x) is subject to rotation (around z), the Coriolis force induces a displacement perpendicular to the initial movement (along y). This displacement makes it possible to deduce the angular velocity as seen in the figure 2:

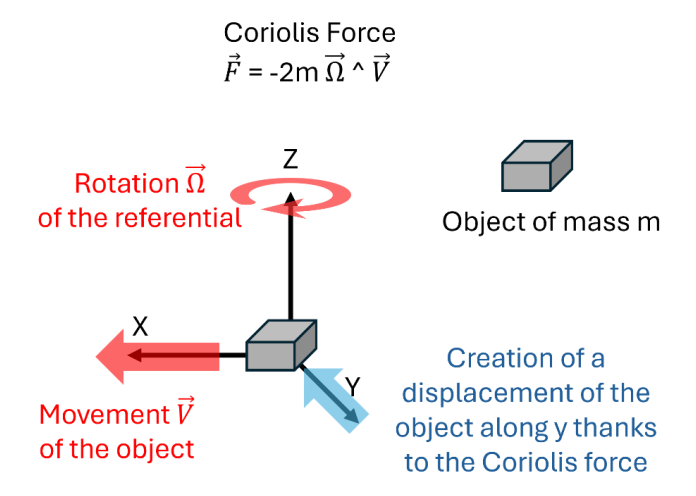


Figure 2: Explanatory diagram of the Coriolis force.

These gyroscopes are generally manufactured using MEMS/NEMS technology, which makes them very lightweight, easily portable, and very small. In addition, their manufacturing cost is relatively low (when industrialized), and they have very low power consumption. However, they are generally less accurate than optical gyroscopes, being sensitive to noise and thermal drift.

2. Gytrix: A navigation grade gyroscope

The GYTRIX (Trigonal quartz crystal gyroscope) gyroscope is a device currently being developed by the CMT team. This innovative MEMS-type gyroscope exploits the piezoelectric properties of natural quartz and an axisymmetric structure. (Thomas Perrier, 2022)

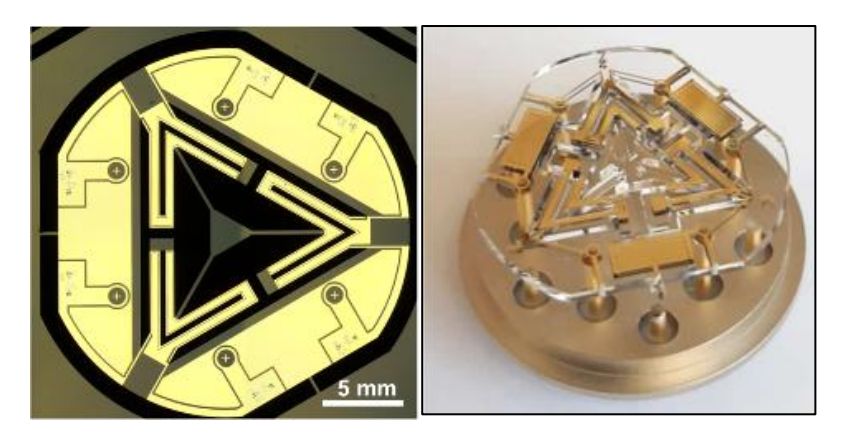


Figure 3: Photos of the Gytrix gyroscope taken by the CMT team. (Thomas Perrier, 2022)

The GYTRIX (figure 3) relies on the piezoelectric effect of quartz: this material becomes electrically charged when subject to mechanical stress. Therefore, the gyroscope can detect and transform mechanical vibrations into electrical signals. The GYTRIX cell is cut from quartz along its crystallographic axes, which allows for a symmetrical structure of three arms of a "Y" shape. This allows for thermal stability and mechanical isotropy. One major advantage of the gyroscope is its very high-quality factor, which can reach several hundred thousand.

The symmetrical structure of the GYTRIX generates two vibration modes with very close frequencies; the two modes can be seen on the figure 4. The gyroscope is composed of three "y" branches and a central mass connected to the branches. Depending on the excited modes, the branches move differently, moving the mass in a different direction, highlighted by the red arrow.

- The "Drive" mode is where one of the arms is stationary; this is the mode initially excited by an oscillator at its natural frequency.
- The "Sense" mode is where all three arms vibrate in response to angular acceleration.

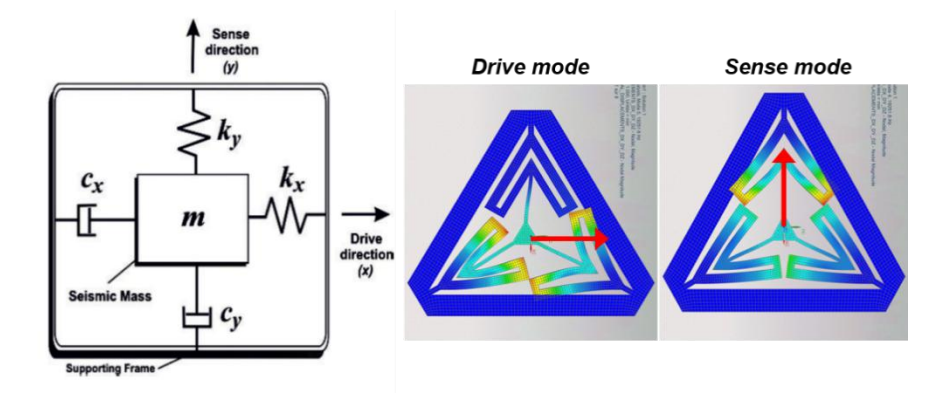


Figure 4: On the left, a schematic representing the behaviour of the Gytrix gyroscope with the two Drive & Sense modes. On the right, a representation of Drive and Sense mode, the scale is in mm, showing the displacement of the Y branches.

The gyroscope Gytrix and its two modes can be described using a mass-spring scheme as a resonator. The mass m represents the central mass of the gyroscope. The group with the spring c_x , k_x represents the functioning of the Drive mode, with x, being the direction of the displacement of the mass when the Drive mode is acting. On the orthogonal direction, as expected due to the Coriolis force, another group of damping-spring c_y , k_y is also acting on the central mass m, representing the Sense Mode, creating a displacement of the mass m in the y direction. The equation (1) describes the behaviour of the gyroscope, using the schematic in figure 4, where the action of the Coriolis force is highlighted in red. The figure 5, show the displacement of the two modes when the gyroscope is under an out-of-place rotation Ω .

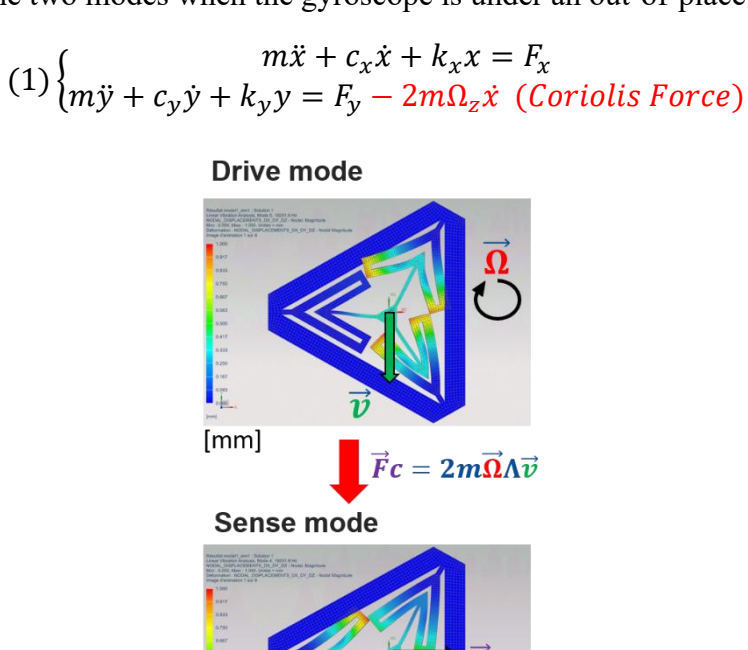


Figure 5: Behaviour of the Drive and Sense modes when the gyroscope Gytrix is under rotation.

[mm]

In the presence of an out-of-plane angular velocity, the Coriolis force acts, and the amplitude of the Sense mode is then proportional to the rotational speed, thus allowing its measurement.

The excitation and detection of Drive and Sense modes are achieved using electrodes arranged on the quartz crystal and an electronic architecture implemented with measuring instruments:

- Drive mode: A voltage is applied to one electrode and the return signal is recovered from another, via a current-to-voltage converter. Closed-Loop Drive Mode Operation: A PLL (Phase Lock Loop) and a PID (Proportional Integrator Derivation) are implemented in Drive mode signal to control the Drive mode signal's frequency and amplitude.
- Sense mode: The electrodes detect the Coriolis signal, amplified differently and compared to the drive signal via synchronous demodulation to produce an output proportional to the rotation.

<u>Using the PLL:</u> To operate the gyroscope, which is a resonator, the gyroscope's Drive mode must be excited at its resonant frequency. This provides the greatest possible response. To do this, an excitation signal is sent, with a frequency equivalent to the Drive mode's resonant frequency. However, the resonant frequency varies over time depending on external environmental conditions, such as temperature. The PLL keeps the Drive signal at resonance by applying a -90° setpoint to the signal's phase. To keep the signal at this phase, the excitation will change frequency and keep the Drive signal frequency at -90°.

<u>Using the PID:</u> Implementing a PID on the amplitude of the Drive signal demodulated at the PLL frequency keeps the amplitude of the Drive signal constant. This makes the Sense signal more stable and improves the quality of the Coriolis signal. To respect this setpoint, the PID will vary the amplitude of the excitation signal.

The PLL and PID constitute the closed loop in Drive mode, changing the excitation signal to meet the requirement of the PLL and PID. In this configuration, it is possible to get the Coriolis signal from the Sense mode real part signal (Figure 6).

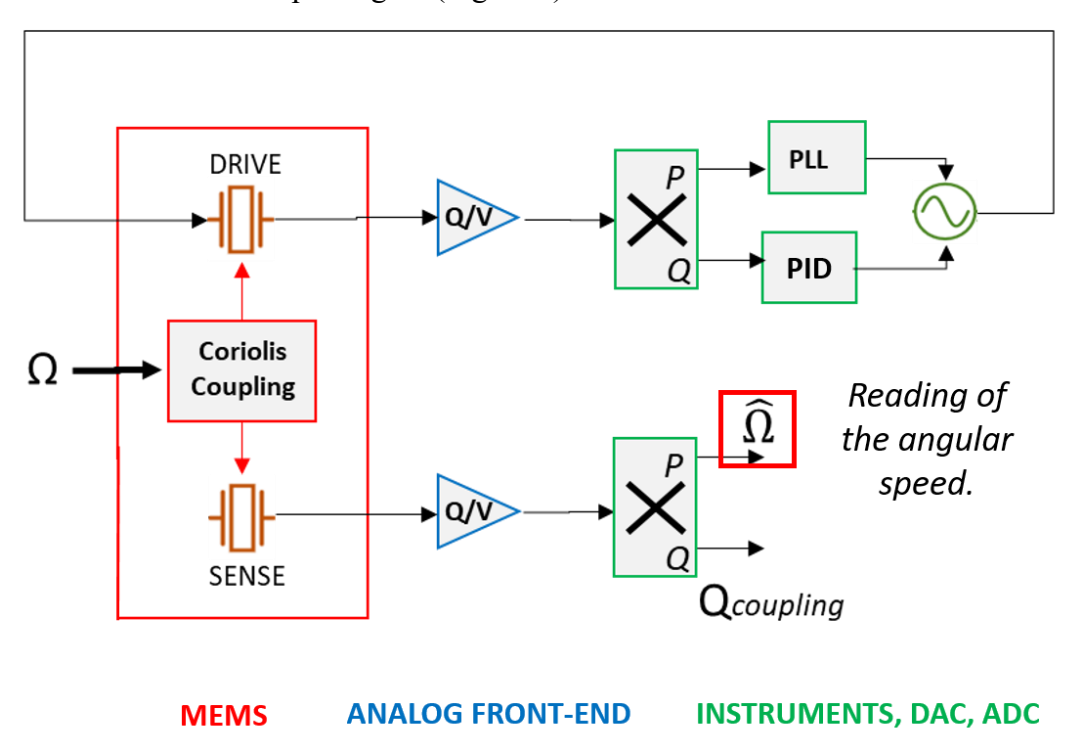


Figure 6: Scheme showing the electronical configuration of the gyroscope to be able to read an angular rate.

Since the GYTRIX uses piezoelectric technology, it requires a proximity electronic circuit to convert the charges generated by the sensor into an electrical signal that can be processed by measurement instruments. The charges produced are first transformed into a readable signal using a current-to-voltage converter. Among the different signals, only the Sense signal is amplified - by a factor of 10 - to improve measurement precision by enhancing the readability of its variations (which are smaller than the Drive mode signal, because it is not at his resonant frequency).

The Coriolis signal is read from the real part of the Sense signal, which will vary when the gyroscope is subject to a rotation speed. However, to obtain a truly accurate Coriolis signal, it is necessary to add a transformation to the Sense signal:

(2)
$$\Omega = i.\frac{\underline{X_S} - \underline{B_S}}{SF}$$

Where $\underline{X_S}$, $\underline{X_D}$ represent the complex signal of the Sense and Drive modes. SF is the scale factor in V_Sense/(°/h)/V_Drive and $\underline{B_S}$, $\underline{B_D}$ represent biases present in the gyroscope. The use of such a scale factor allows a better precision on the angular rate reading because it allows the Coriolis signal to be correctly extracted independently of external variations in the Drive and Sense signals.

To conclude, this section explained the functioning of the GYTRIX gyroscope going from the mechanical behaviour of the structure to the role of the proximity board to read the signals. The figure 7 is a picture of the GYTRIX vacuum-sealed (to avoid any damping with gas and to maximize the quality factor) in its copper case with on top, the proximity board.

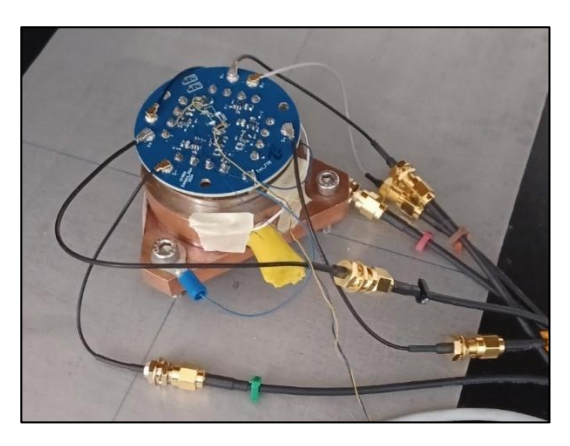


Figure 7: Image of the GYTRIX gyroscope vacuum-sealed in the copper case with its electronic board attached to it.

3. Allan Variance (Characterization tool)

During this internship, I often used the Allan variance tool to estimate the stability over time of the gyroscope and quantify its accuracy. It also allows me to determine the best measurement time to obtain the least noisy signal possible in record times.

The Allan variance is a mathematical quantity frequently used to estimate the stability over time of the frequency of any oscillator. Allan variance is a fundamental tool for analysing the stability of time-domain signals from physical sensors. The term is Allan variance, but it is actually the standard deviation used as unit, the physical quantity is °/h. (DELAHAYE, 2021)

The calculation for an Allan variance is as follow:

$$(3) \sigma_s^2(\tau) = \frac{1}{2} \langle (y_{n+1} - y_n)^2 \rangle$$

Where y_n are the successive samples of frequency deviations and τ is the sampling step. The relationship with the variable τ makes it possible to distinguish the causes of instabilities based on their impact on the measurement in the short, medium, or long term.

Several types of noise are characterized on an Allan variance:

Noises	$\sigma(\tau)$ slope (log)	Origin:	$\sigma^2(au)$ coefficients
Deterministic Noise	+1	Environmental variations. (predictable)	Depends on the environment
Red Noise	+1/2	Random Walk of the signal.	$\frac{2.\pi^2}{3} \cdot \varsigma_{-2} \cdot \tau$
Pink Noise	0	1/f noise, instability bias of the instrument.	$2.\ln(2).\varsigma_{-1}$
White Noise	-1/2	Random noise. (unpredictable)	$\frac{1}{2} \cdot \varsigma_0 \cdot \tau^{-1}$
Violet / Blue Noise	-1	Derived from white / pink noise.	$\frac{3.\gamma - \ln(2) + 3.\ln(2.\pi.f_c.\tau)}{4.\pi^2}.\varsigma_1.\tau^{-2} + \frac{3.f_c}{4.\pi^2}.\varsigma_2.\tau^{-2}$

Table 1: Types of noises in an Allan variance in time domain, with f_c the high-cutoff frequency of the physical system studied, $\gamma \cong 0.577$, the Euler-Mascheroni constant and $\tau \gg \frac{1}{2.\pi.f_c}$. (DELAHAYE, 2021)

The figure 8 shows the different types of noise in an Allan variance:

Allan Variance

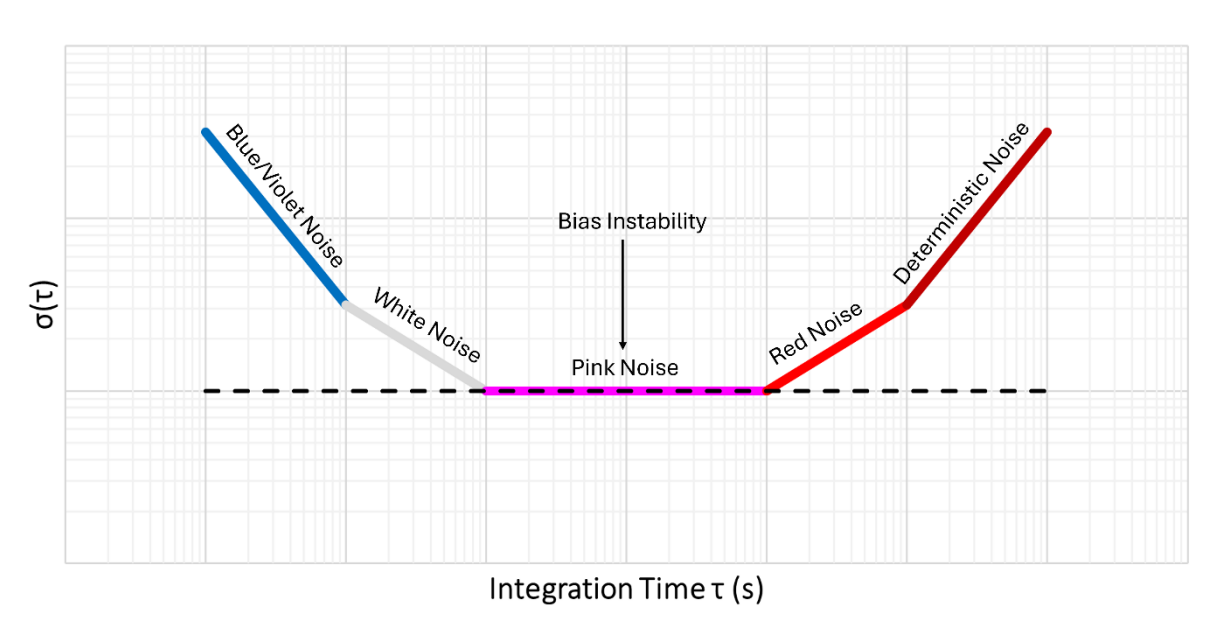


Figure 8: Presentation of Allan Variance showing the types of noise present in a gyroscope.

Therefore, with an Allan variance of this form, it is preferable to choose an integration time that corresponds to the intersection between the white noise segment and the pink noise segment. Choosing a shorter integration time would reduce our accuracy, and using a longer time would not improve our accuracy, only waste time. Characterizing the different noises in the frequency domain will also be useful. There are equations that allow us to transition from one domain to the other. (DELAHAYE, 2021) By using the coefficients of the noise in time domain, it is possible to connect them with the following equations in frequency domain:

(4)
$$S_s(f) = \varsigma_{-2}.f^{-2} + \varsigma_{-1}.f^{-1} + \varsigma_0 + \varsigma_1.f + \varsigma_2.f^2$$

In the equation 4, S_s is the power spectral density of the gyroscope variance. The different noises form the figure 9 in the frequency domain:

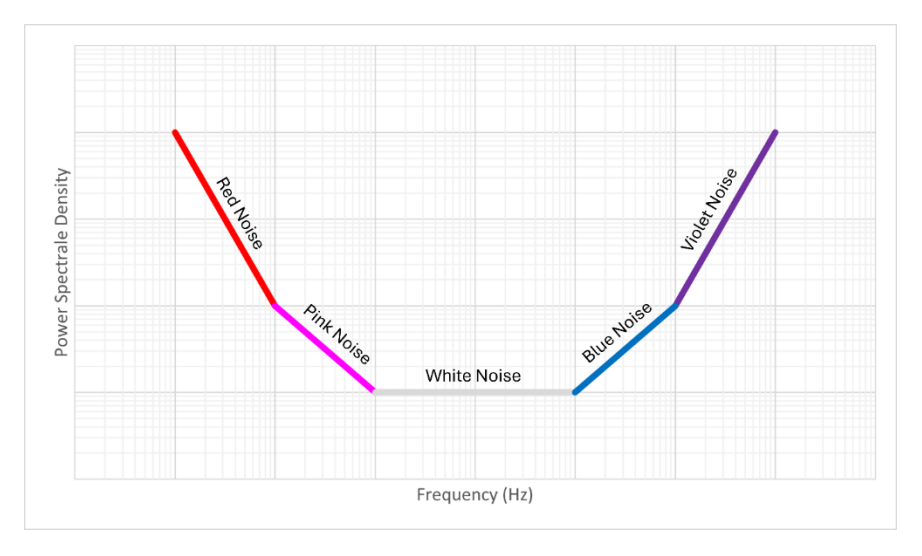


Figure 9: Presentation of Allan Variance in the spectral domain showing the types of noise present in a gyroscope.

The figure 10 is a measure of Allan variance I did during the internship. This is a 5 min noise acquisition, and it allowed me to control the precision of the gyroscope.

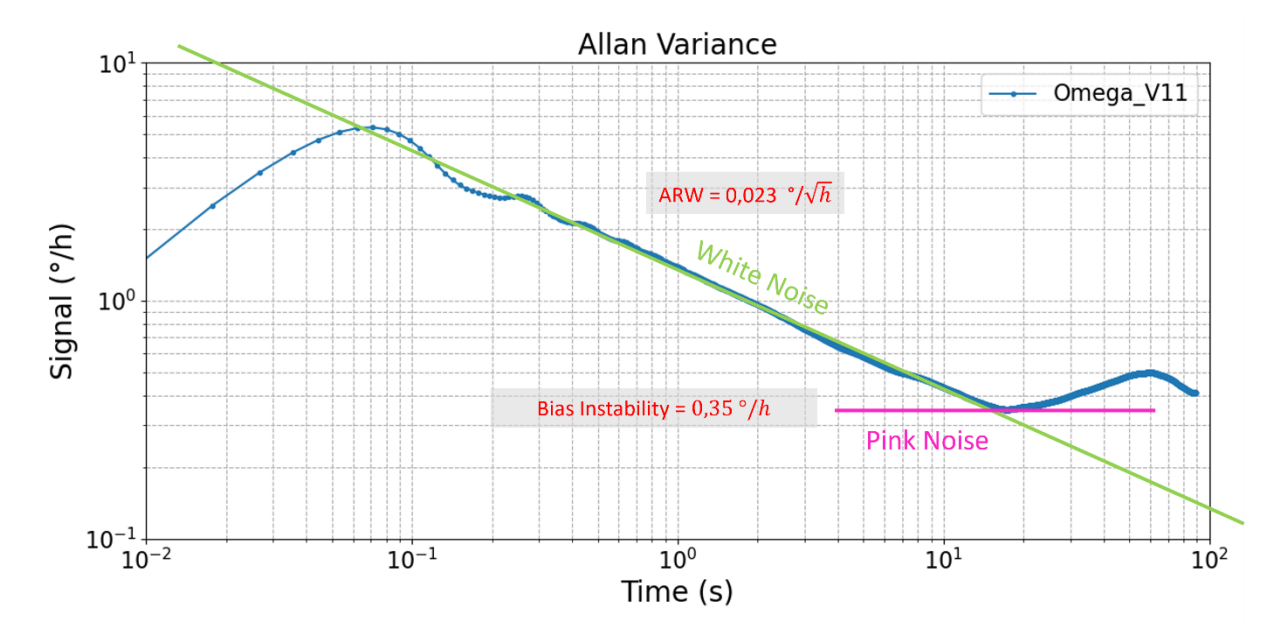


Figure 10: Allan variance of the V11 model, the red line has a slope of -1/2 representing white noise; the flat line is the one representing pink noise.

This Allan variance shows that the maximum resolution achievable with this instrument is 0.35° /h for an integration time of approximately 15 seconds and an ARW (Angle Random Walk) from white noise, of 0.023° /h. We clearly observe a straight line with a slope of ½ which corresponds to the white noise when we display the curve with the standard deviation. This value shows that the gyroscope can achieve such accuracy, which should be sufficient to measure the rotation speed of the Earth, which is a signal of amplitude of 15 °/h, which is converted in 0.004° /s! Successfully carrying out such an experiment would prove the accuracy of the gyroscope!

4. Nyquist Circle (Characterization tool)

When I explained the transformation of the Sense signal into a Coriolis signal (p.13), I used two biases: $\underline{B_S}$ and $\underline{B_D}$ without initially detailing their origin. These biases come from the analysis of Nyquist circles; a tool used for gyroscope characterization. Unlike the Bode plot, which separates the representation of modulus and phase on two distinct graphs, the Nyquist plot allows these two pieces of information to be visualized simultaneously on a single complex plane: the phase being represented by the angle relative to the origin, and the modulus by the distance from the point to the origin. In our case, the Nyquist plot is used to extract and verify several gyroscope parameters: the resonance frequency, the quality factor, as well as mechanical or electrical couplings referenced as $\underline{B_S}$ and $\underline{B_D}$. Considering these biases is essential to improve the accuracy of Coriolis signal measurement!

Two types of unwanted coupling can be observed on the Nyquist diagram, each affecting the representation of the circle differently!

The first physical effect observed is mainly due to capacitive coupling, resulting from the proximity of the copper threads on the circuit board. At the resonant frequency, the gyroscope is theoretically expected to exhibit a zero-phase signal and a maximum quadrature signal. However, this capacitive coupling introduces a parasitic component into the Drive signal, preventing it from being perfectly zero, even when the gyroscope is not subject to rotation. This situation arises a problem when we need to adjust the resonator phase. Due to the shift introduced by the capacitive coupling, this positioning no longer corresponds to the true resonance of the gyroscope. The system then becomes slightly out of phase, which affects the precision of the measurement. To correct this phenomenon, it is necessary to precisely characterize this angular shift, to be able to inject it as a demodulation phase to counter the effect. The gyroscope is now really at its frequency resonance. This phenomenon creates a shift in the circle with respect to the origin.

The second phenomenon affecting the diagram is related to the charge amplifier integrated into the electronic board. This introduces a phase shift into the signal, resulting in a rotation of the Nyquist circle. This rotation modifies the angular position of the system's response and must be considered to ensure correct reading of the gyroscope parameters.

Those two unwanted couplings justify the utilisation of Nyquist Circle to deduce $\underline{B_S}$ and $\underline{B_D}$ and make precise measurements. To construct the Nyquist circle, we need five measurements of the Drive and Sense signals that are described in the table 2. In order to construct it, I developed a Python script that automatically run the measurements and analyse the results to extract the parameters of interest. (DELAHAYE, 2021) $\underline{B_S}$ and $\underline{B_D}$ are extracted by averaging the measurements off-resonance and correspond to the combined effect of unwanted couplings. This is why they are subtracted during the extraction of the Coriolis signal, as described in equation (2).

PLL Setpoint	Description:
during the measure	
-90°	Measurement when the gyroscope is at resonance.
-45°	Measurement when the gyroscope is at -3dB before resonance.
-135°	Measurement when the gyroscope is at -3dB after resonance.
Off	Measurement when the gyroscope is off-resonance and the
	measurement frequency is smaller than the resonance frequency.
Off	Measurement when the gyroscope is off-resonance and the
	measurement frequency is greater than the resonance frequency.

Table 2: Description of the different points necessary for the construction of a Nyquist circle.

Once the five measurements are realized, the script create a fit for the Drive and Sense. In the figure 11, the big red circle corresponds to the response of the Drive mode and the smaller orange circle, to the response of the Sense mode. The blue and orange points are the measurements points, and the purple point is the identified resonance point. After the first circle, the parameters in the instrument settings are updated to consider the coupling calculated and a Nyquist circle is measured again to see the effect on the measurements. This can be seen on the figure 11, the first picture on the left, is the first circle, the picture on the right is the measured circle after the update of the instrument settings.

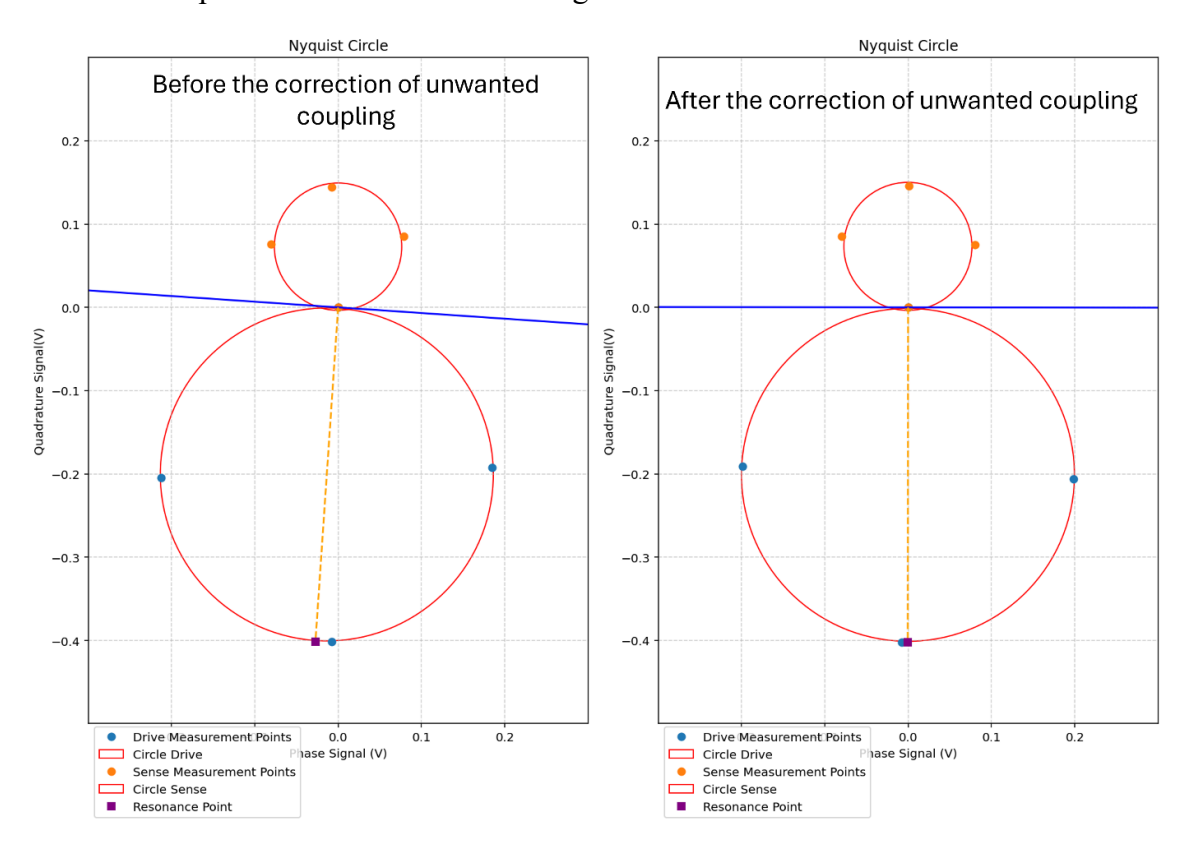


Figure 11: Two successive Nyquist circles showing the effects of unwanted couplings and the effects of the corrections made.

So, the reading of the Coriolis signal is now complete, the two biases $\underline{B_S}$ and $\underline{B_D}$ have been identified and corrected. The next step is to describe the North Finding experiment!

5. North Finding Presentation

Measuring the Earth's rotational speed is essential in the North Finding experiment. This experiment involves orienting a local reference with respect to the geographic North by measuring the Earth's rotational speed in different directions to recreate the Earth's rotational speed sinusoid. A graphic representation is available in figure 12:

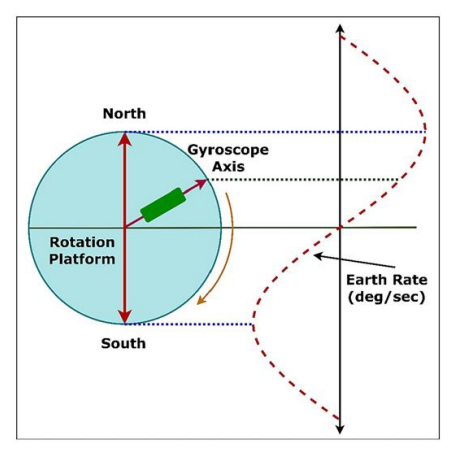


Fig. 13. Sinusoidal output of Gyroscope as Earth's Rotation Rate in horizontal plane [94].

Figure 12: Explanatory diagram of the North Finding measurement, from (Asif, 2024).

Indeed, the value of the Earth's rotational speed is fully measured when the sensitive axis of the gyroscope is oriented in the direction geographic north. In this case, the gyroscope measures +15°/h, the value of the Earth rotational speed. If the gyroscope is oriented south, it measures -15°/h, as it is be oriented in the opposite direction. When oriented east or west, the gyroscope will measure 0°/h. Measuring this signal accurately, despite the presence of various noises (thermal, gravitational, electronic, etc.), constitutes proof of the quality of the gyroscope used. To set up the North Finding experiment, there are two methods: Maytagging, the static method, and Carouseling, the dynamic method. These two approaches make it possible to separate parasitic physical effects (bias, gravity, thermal drifts) from the desired signal.

a. Maytagging Method

The Maytagging method is a static method consisting of taking successive measurements at two opposite orientations, for example, 0° and 180°. This compensates for constant biases (sensor bias and gravitational bias assumed to be constant over short periods) and extracts the true signal of Earth's rotation. This method is easy to implement. Stepper motors allow for high orientation accuracy and reduce associated errors. Usually in literature, measurements are done horizontally on a table, meaning that the measurement of the Earth's rotational speed is a measurement of the projection of the Earth's projection speed at horizontal level, at the local latitude. The measurements made by the gyroscope are of the form:

(5)
$$\omega_{0^{\circ}} = \Omega_E . \cos(\varphi) \cos(\Psi - \theta) + b + b_g$$

(6)
$$\omega_{180^{\circ}} = -\Omega_E \cdot \cos(\varphi) \cos(\Psi - \theta) + b + b_g$$

With $\omega_{0^{\circ}}$, $\omega_{180^{\circ}}$ the rotation speeds measured by the gyroscope at the specified orientation in the reference frame. Ω_E is the value of the Earth's rotation speed and θ is the angle between the geographic North and the local reference frame. The angle φ corresponds to the latitude; the angle Ψ corresponds to the orientation angle of the gyroscope in its local reference frame. Finally, b_g corresponds to the bias generated by gravity, modeled as a constant term if the gyroscope says horizontally on a table, and b corresponds to other biases of the gyroscope, which may not be constant. It is possible to minimize the impact of these biases by assuming that their characteristic times are greater than that of the measurement. This allows them to be assumed equal during a measurement and its opposite measurement, so that they cancel each other out during the subtraction of the equation (5) and (6):

$$(7) \Omega_E.\cos(\varphi)\cos(\Psi-\theta) = \frac{\omega_{0^{\circ}} - \omega_{180^{\circ}}}{2}$$

This method allows us to obtain an estimate of the desired signal, without the influence of bias.

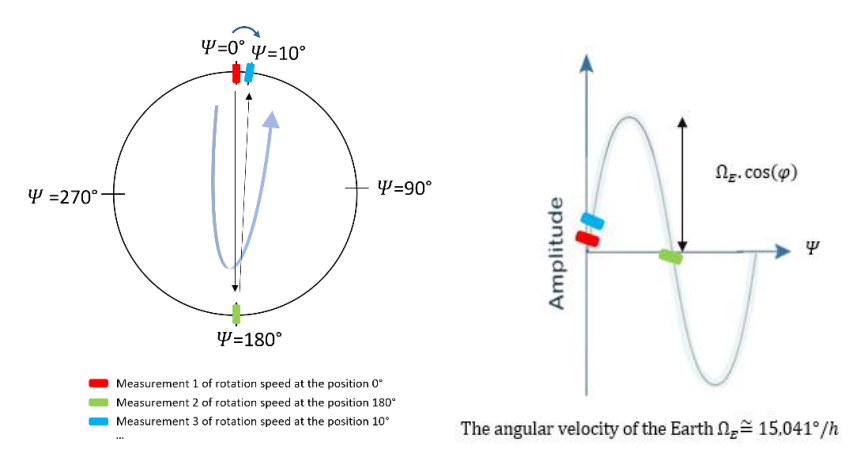


Figure 13: Explaining the Measurement Process Using the Maytagging Method.

The figure 13 explains the process of a North Finding measurement using the Maytagging method. The figure on the left shows the orientation of the gyroscope in a local reference frame, and the one on the right places the measurements on the Earth's rotational velocity sinusoid. In this configuration, the local plane is aligned 90° left of North, which is the angle where the sinusoid is maximum. The first measurement is taken at 0°, and the next is its opposite at 180° in the reference plan. The gyroscope shifts 10° between each measurement pair (in this configuration) and repeats its measurement at 10° and its opposite at 190°, and so on until it completes a 360° rotation. The diagram on the right shows where the measurements are taken on the Earth's rotational velocity sinusoid.

b. Carouseling Method

The Carouseling method is a dynamic method that involves measuring rotational speed continuously by rotating one complete revolution at a constant speed. This technique relies on modulation of the Earth's rotational speed (which is constant) to separate biases, scaling factors, and temperature errors. It requires precise continuous rotation. The key assumption is that biases evolve slowly compared to the rotation period, which allows them to be considered constant over a complete revolution (figure 14):

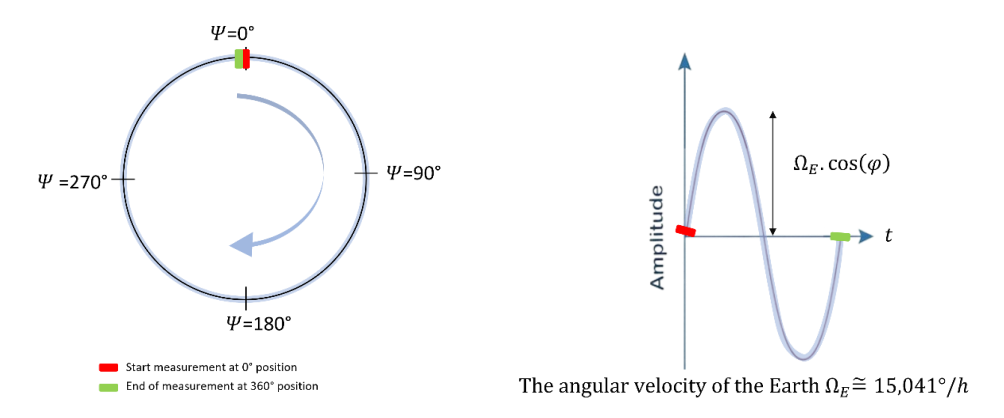


Figure 14: The diagram on the left shows the path taken by the Carouseling method, which completes a 360° rotation at a constant speed. The diagram on the right shows what the gyroscope measures: a continuous sinusoidal signal of the Earth's rotational speed.

However, this method was not implemented because it requires the use of a continuous motor, and only a stepper motor was available, which would have made a lot of noise during rotations. Instead of implementing a continuous Carouseling, this method was slightly changed to implement a discrete Carouseling. The gyroscope follows the same path as in a continuous Carouseling, but it makes discrete measurements (figure 15):

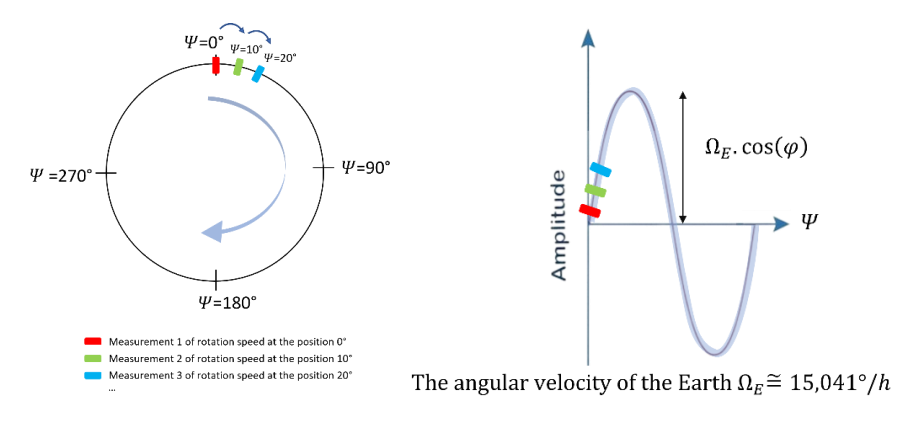


Figure 15: The diagram on the left illustrates the path followed by the carousel method, which makes discrete measurements over 360°. The diagram on the right illustrates what the gyroscope measures: a sinusoidal signal reconstructed from discrete measurements of the Earth's rotational speed.

The equation (8) shows the form of the angular velocity measured using the Discrete Carouseling method, using the same variables names as for equation (5), (6), (7):

(8)
$$\omega = \Omega_E. cos(\varphi). cos(\Psi - \theta) + b + b_g$$

This method allows us to take advantage of the measurement integration time and thus avoid having a noisy signal due to electronics, the environment, and motor vibrations.

The North Finding experiment illustrates the ability of modern gyroscopes to detect an extremely weak signal: the Earth's rotation one!

6. Data Simulator Presentation

During the literature review on North Finding, there were many configurations present. The question of what the best configuration was arose. To describe the different possible configurations, . But the best configuration for one gyroscope is not necessarily the same as another with a different Allan variance. That's why I set up a simulator that generates a noisy gyroscope signal based on its Allan variance. This allows me to explore the different measurement possibilities offered by the gyroscope and determine the configuration that seems to produce the most accurate results. The goal of this data simulator is to explore the different possible Maytagging or Carouseling configurations to determine which one yields the best results. This simulator is based on the Allan variance, which describes how the gyroscope noise evolves over time.

The method consists of:

- Reproducing the Allan variance from the gyroscope specifications and converting it into a spectral domain filter.
- Filtering the white noise (flat spectrum) with the spectral domain filter.
- Generating a noisy time-domain signal.
- Splitting the time-domain signal according to the type of scenario used.
- Superimposing this synthetic noise on a simulated Earth rotation signal representing the measured component.
- Using the measured data and transforming it to extract the sinusoid of the Earth's rotational speed.
- Extracting the angle corresponding to the North orientation.

Thus, to simulate the noise generated by a gyroscope, everything starts with its Allan variance! To recreate the Allan variance of a gyroscope in the data simulator, a few simplifying assumptions were made: the Allan variance contains only three major noises: white noise, pink noise, and noise from the environment. This simplifies the form of the Allan variance, which can be described with three parameters:

- σ_{min} : The value of the instability threshold and therefore the maximum precision that the gyroscope can achieve.
- $\tau a u_1$: The minimum integration time that allows the instability threshold to be reached, after averaging the white noise to the maximum.
- $\tau a u_2$: The maximum integration time that allows the instability threshold to be reached before the noise increases again due to environmental noise drifts.

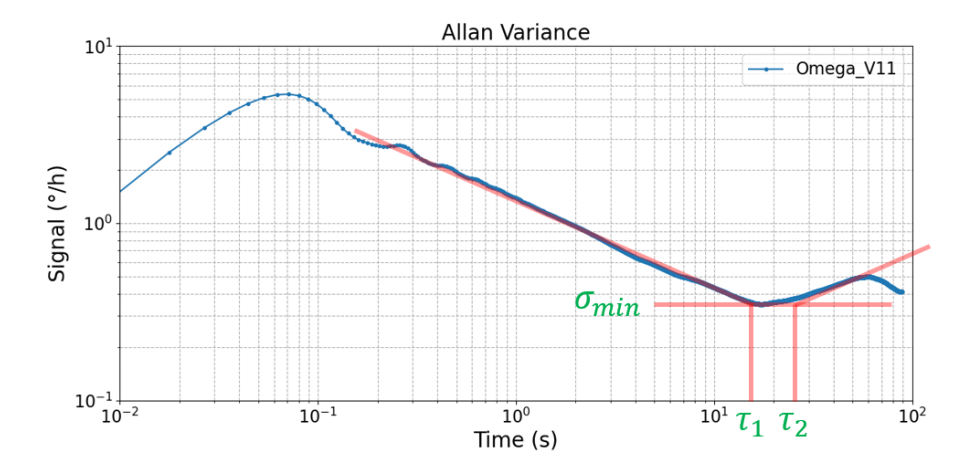


Figure 16: Visualization of σ_{min} , $\tau \alpha u_1$, $\tau \alpha u_2$ on the measured Allan variance done in 5 min measurement.

In the Allan Variance in the figure 16, the three parameters are:

- $\sigma_{min} = 0.35 \,^{\circ}/h$
- $\tau a u_1 = 15s$
- $\tau a u_2 = 25s$

To generate the gyroscope noise, it is necessary to convert the Allan variance into the frequency domain using the noise power spectral density. Having simplified the form of the Allan variance, the spectral density is also simplified:

$$(9) \sigma_s^2(\tau) = \frac{2 \cdot \pi^2}{3} \cdot \varsigma_{-2} \cdot \tau + 2 \cdot \ln(2) \cdot \varsigma_{-1} + \frac{1}{2} \cdot \varsigma_0 \cdot \tau^{-1}$$

$$(10) = S_s(f) = \varsigma_{-2} \cdot f^{-2} + \varsigma_{-1} \cdot f^{-1} + \varsigma_0$$

It is possible to estimate $\zeta_0, \zeta_{-1}, \zeta_{-2}$ starting with τ_1, τ_2 and dev:

(11)
$$\begin{cases} \varsigma_{-1} = \frac{dev^2}{2} \cdot \ln(2) \\ \varsigma_{-2} = 2 \cdot \ln(2) \cdot \frac{\varsigma_{-1}}{2 \cdot \pi^2} \cdot \frac{\tau_2}{3} \\ \varsigma_0 = 2 \cdot \ln(2) \cdot \varsigma_{-1} \cdot 2 \cdot \tau_1 \end{cases}$$

From the calculated coefficients, it is possible to obtain the form of the power spectral density of the Allan variance, as seen in figure 17:

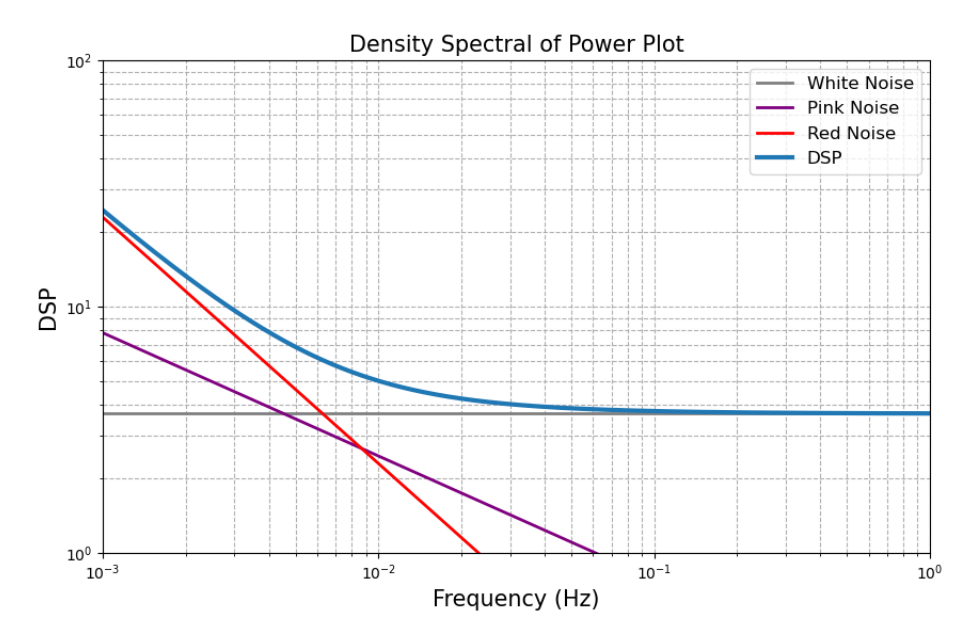


Figure 17: Power spectral density of the Allan variance in the spectral domain, constructed from the equations above.

Using the spectral density of the Allan variance as a filter superimposed on white noise, the signal obtained is passed through a Butterworth low-pass filter of order 2 and cut-off frequency 9 Hz to compare the simulated signal and that at the output of the measuring instruments, emitted by the gyroscope (figure 18):

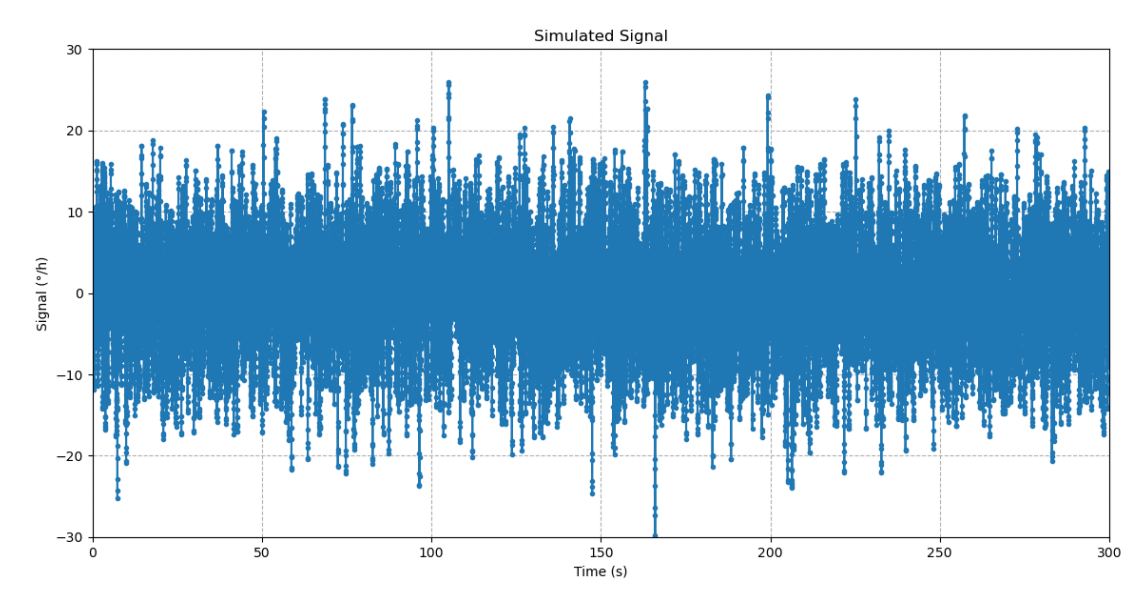


Figure 18: Simulated noise from white noise.

This signal is a signal that could be emitted by the gyroscope with the corresponding Allan variance. It is a 300s sample, directly converted into degree-per-hour (°/h), the unit of measurement that interests us. It is possible to compare this with a signal measured by this gyroscope, in the figure 19:

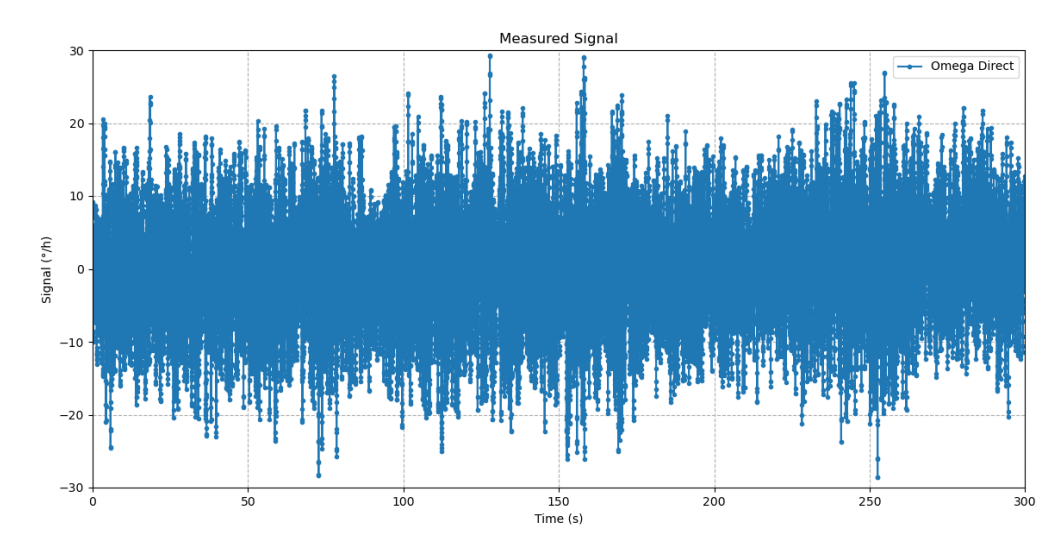


Figure 19: Measured noise from the V11 gyroscope.

To compare the two signals, it is useful to recalculate the Allan variance and an FFT to visually compare the two signals. Both the FFT and the Allan variance display the same information but in different ways, in figure 20 and 21:

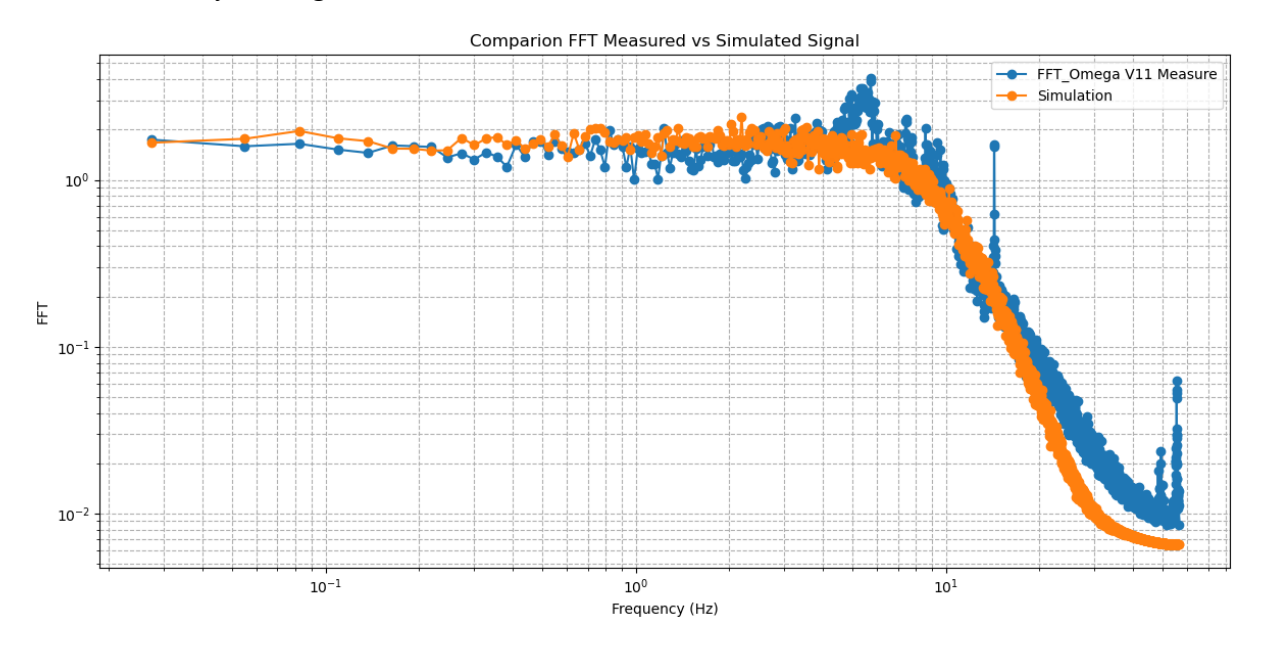


Figure 20: FFT of measured and simulated signals.

The FFT (Fast Fourier Transform) gives a result similar to the measured signal! There are frequencies that are not there, and that I have not added because these are frequencies that will likely disappear with the evolution of Gytrix technology or are from undetermined environment source that may disappear in the future.

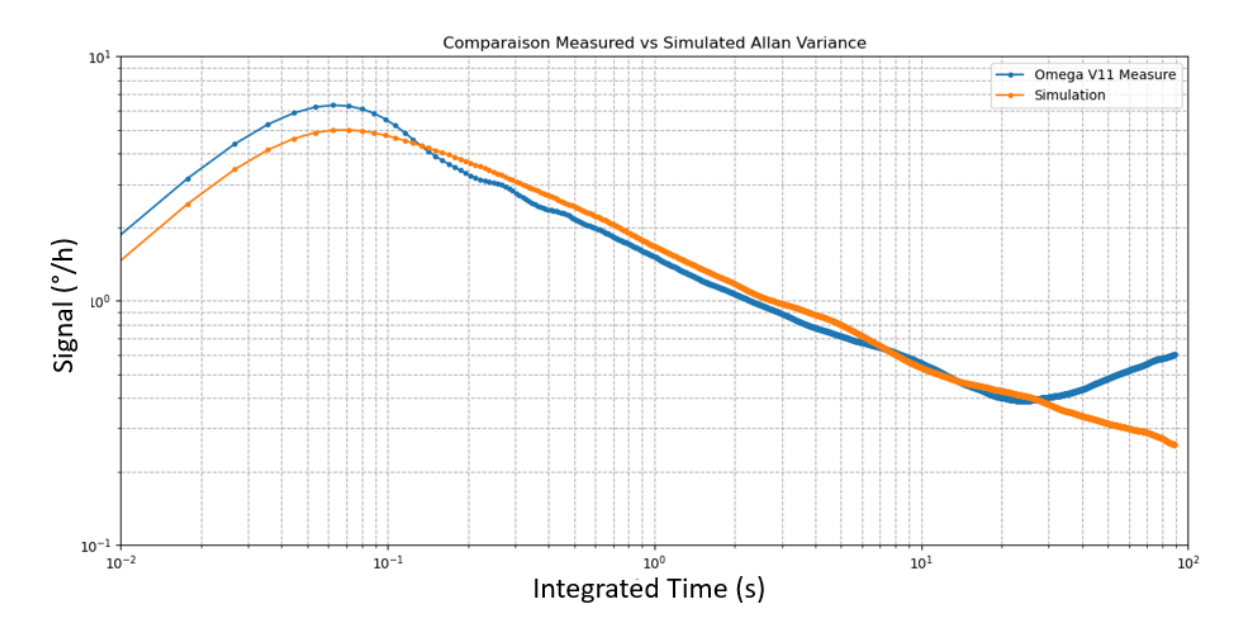


Figure 21: Allan Variance of simulated and generated signals.

The two signals appear to have the same Allan variance, with a few minor differences: it's normal for the orange curve not to rise, because the rise of the curve depends on the external environment and its variations, such as temperature, for example, which is modelled as a continuous drift. However, if there is no rise in the Allan variance, this means that the signal can be integrated indefinitely until the desired accuracy is reached. However, this does not work like that, because the longer a signal is integrated, the longer the gyroscope is subject to external environment variations, the less likely it will be possible to obtain a measurement. Without this rise in the Allan variance, the data simulator also becomes meaningless, because it is obvious that long measurements will be favoured. This is why a slow variation in the signal was artificially added to correspond to the rise in the Allan variance of the measured signal, in figure 22:

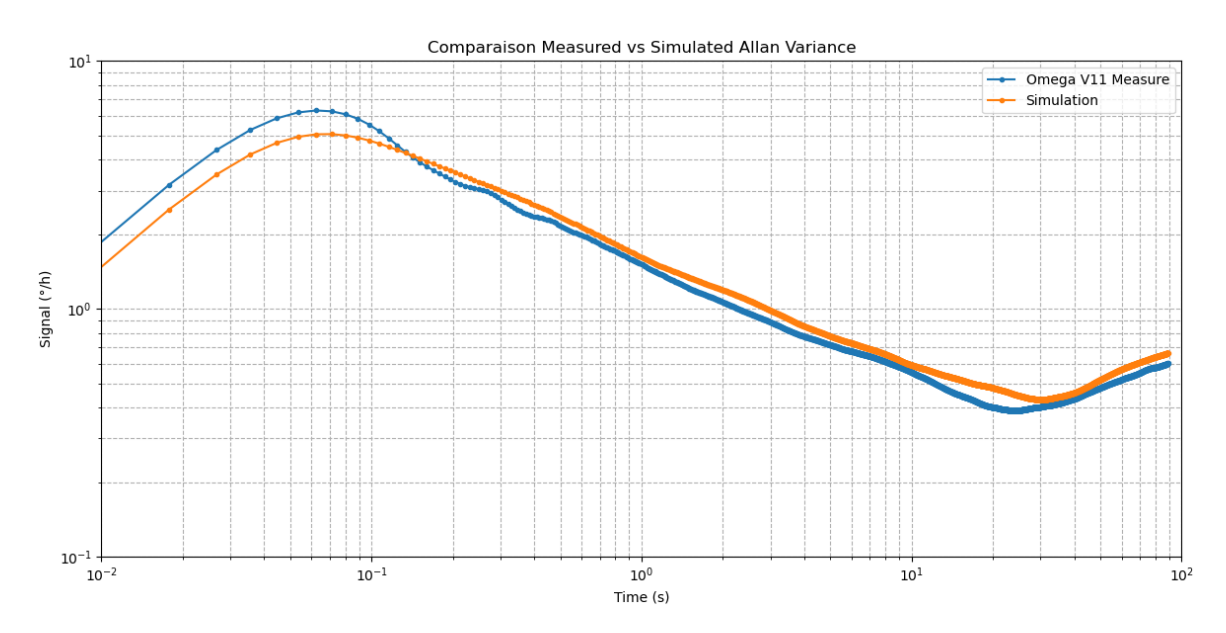


Figure 22: Allan Variance of simulated (artificially modified) and generated signals.

Therefore, with this Allan variance, we can conclude that the first step, consisting of simulating a signal comparable to the gyroscope output signal, is complete. The next step is to use this signal to perform simulations in the context of North Finding. To do this, a script takes the scenario format as a parameter and generates the list of angles at which the measurements will be made. For example, take the scenario $(4,0,1,10)_1$ 0s; the list of angles will be: [0, 10, 20,... 350,350,360,360,350,...10,0, 0, 10, 20,... 350,350,360,360,350,...10,0], which corresponds to a Carouseling taking a measurement every 10° on a round trip.

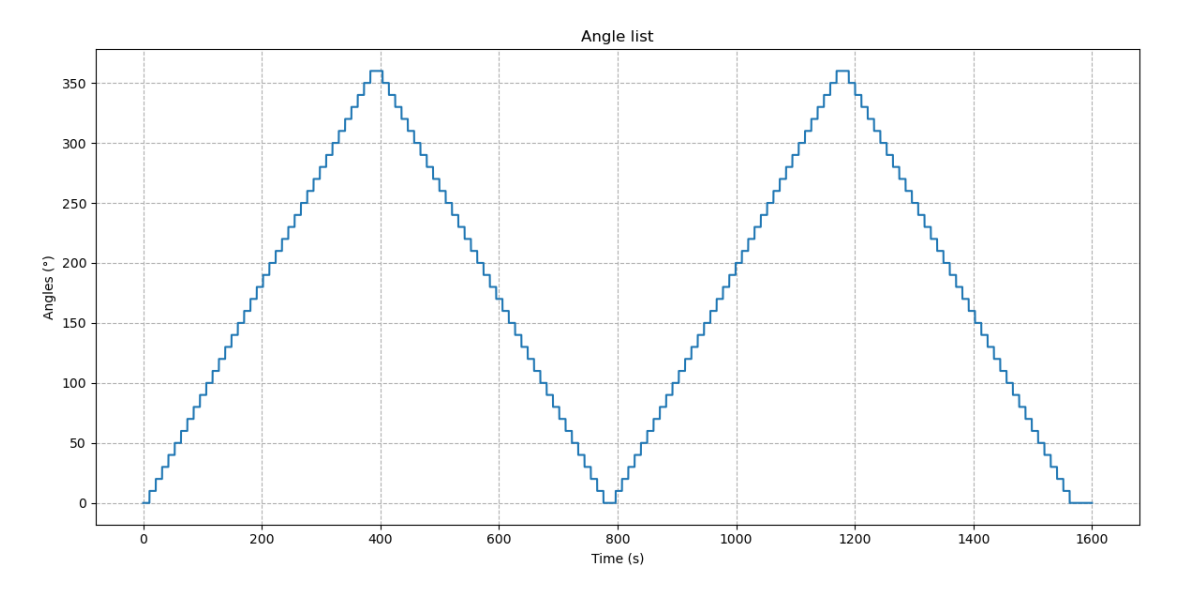


Figure 23: List of angles displayed in graphic form. On the ordinate, the value of the angle at which the gyroscope will be oriented during the measurement, on the abscissa, the corresponding time of the measurement.

This figure 23 represents the passage of angles through which the gyroscope takes measurements. The script considers a total scenario time, here 1600 seconds (around 26 minutes), and a measurement time set to 10 seconds. From the provided scenario details, it calculates the number of measurements and the time allocated to each measurement. It also considers the measurement time "lost" over the total scenario duration when moving from one position to another (here the speed entered is 15.5°/s, which corresponds to the stepper speed).

Knowing the value of the Earth's rotation speed oriented at each measurement angle, it is sufficient to superimpose the value of the Earth's rotation speed projected at the gyroscope's orientation on the previously simulated signal. In this simulation, I chose to orientate the North at 38° from the zero of the local reference frame, as in figure 24.

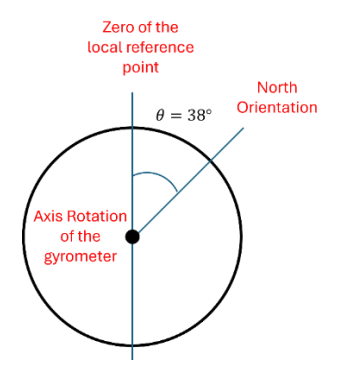


Figure 24: Position of the local reference frame relative to North.

This gives the figure 25:

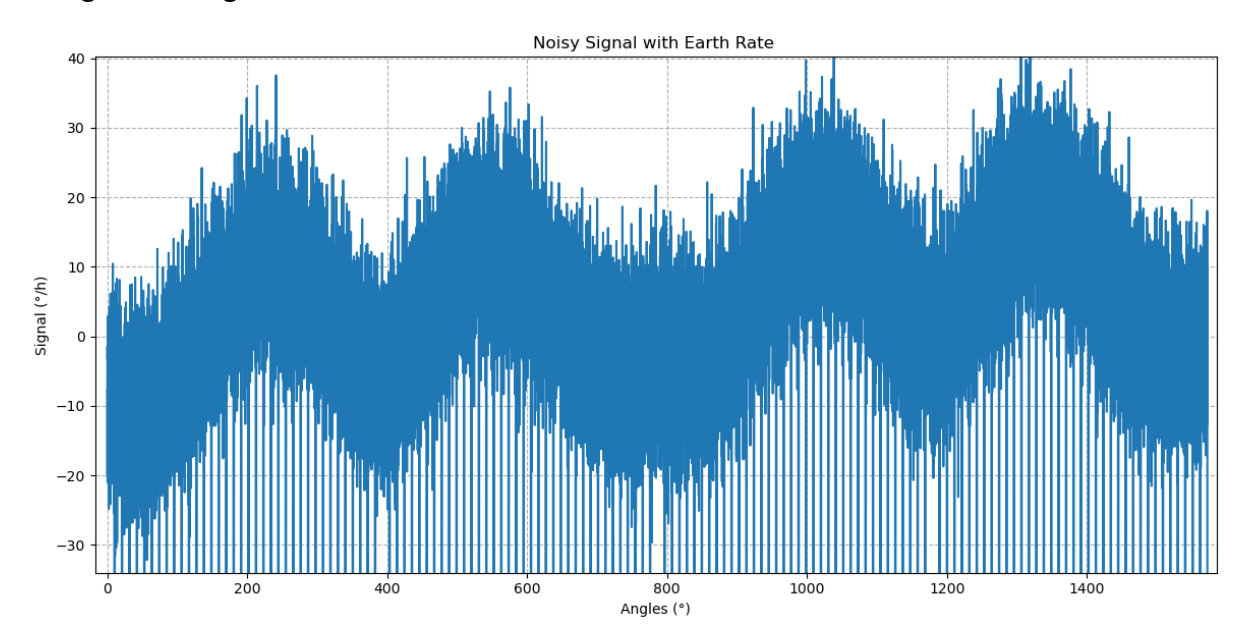


Figure 25: Simulated signal with the addition of the component of the Earth's rotation speed as a function of the gyroscope's orientation relative to North.

Figure 25 shows the Earth's rotation signal added to the simulated noisy signal. As seen with the list of angles, the value of the projected Earth rotation speed is superimposed. Part of the signal is indeed lost due to the rotation from one position to another. These signal parts are then averaged to save only the average of these measurements. In figure 26, there is a visible thermal trend in the results, which is explained by the addition of the "thermal signal" to increase the Allan variance.

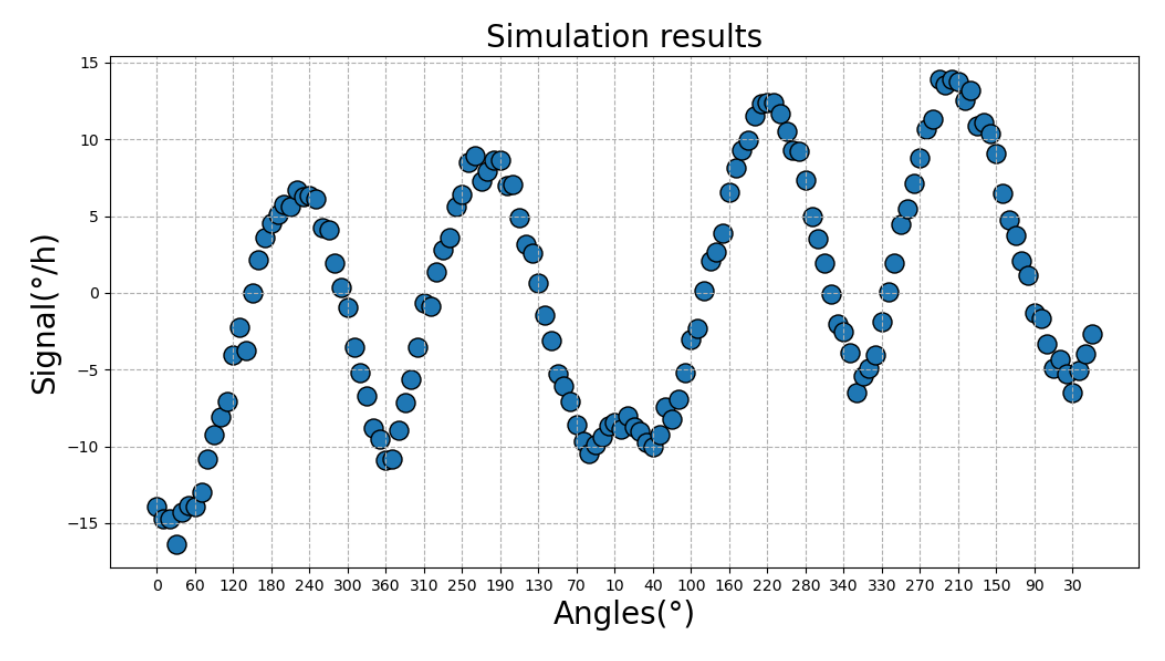


Figure 26: Display of the averaged measurements of the Earth's rotation speed as a function of angle.

The measurements are then sorted and used to extract the value of the angle relative to North, in figure 27.

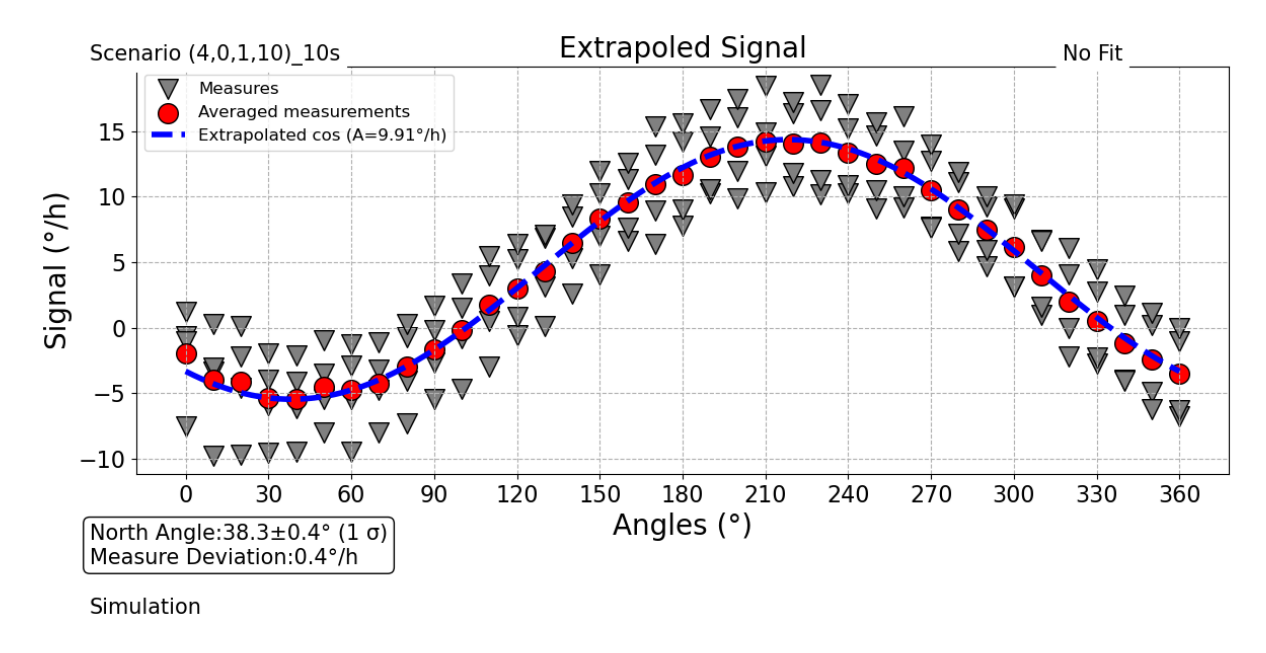


Figure 27: North Finding Simulation. Scenario: (4, 0, 1, 10,)_10s.

Even with the thermal trend, the points compensate each other and allow the script to extract a nice sinusoid with an angle relative to the extracted North of 38.3° and an accuracy of 0.4°.

To improve the accuracy of both simulations and measurements, each scenario was repeated multiple times. For the simulations, 10,000 iterations were performed to achieve a result accuracy of approximately 1%. On average, the Carouseling method estimated the North angle at $38.14~^{\circ}\pm0.33~^{\circ}$, while the Maytagging method yielded an average value of $37.98~^{\circ}\pm0.29~^{\circ}$. However, a closer analysis of the individual measurement points shows that the Maytagging method demonstrates better robustness and consistency. Indeed, the results obtained with Carouseling exhibit greater dispersion, whereas Maytagging provides more tightly clustered measurements, indicating higher repeatability.

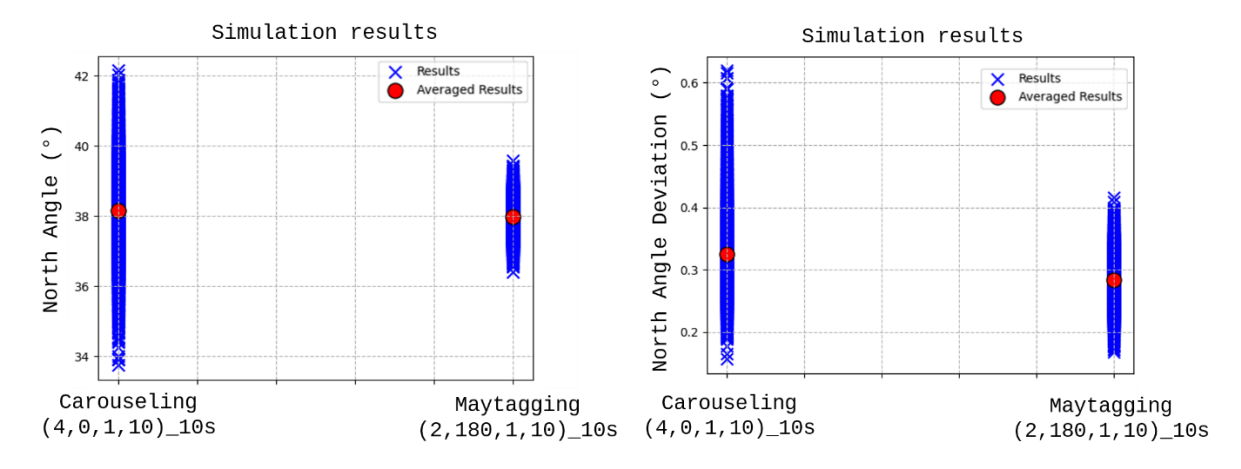


Figure 28: Simulation results of North Finding experience of a Carouseling and a Maytagging.

For the North Finding measurements, the Carouseling and Maytagging methods were repeated three times to evaluate the variability of the results. On average, the Carouseling method estimated the North angle at $38.90^{\circ} \pm 0.96^{\circ}$, while the Maytagging method yielded an average value of $38.40^{\circ} \pm 0.97^{\circ}$. As for the simulation, a closer analysis of the individual measurement

points shows that the Maytagging method demonstrates better robustness and consistency. Indeed, the results obtained with Carouseling exhibit greater dispersion, whereas Maytagging provides more tightly clustered measurements, indicating higher repeatability.

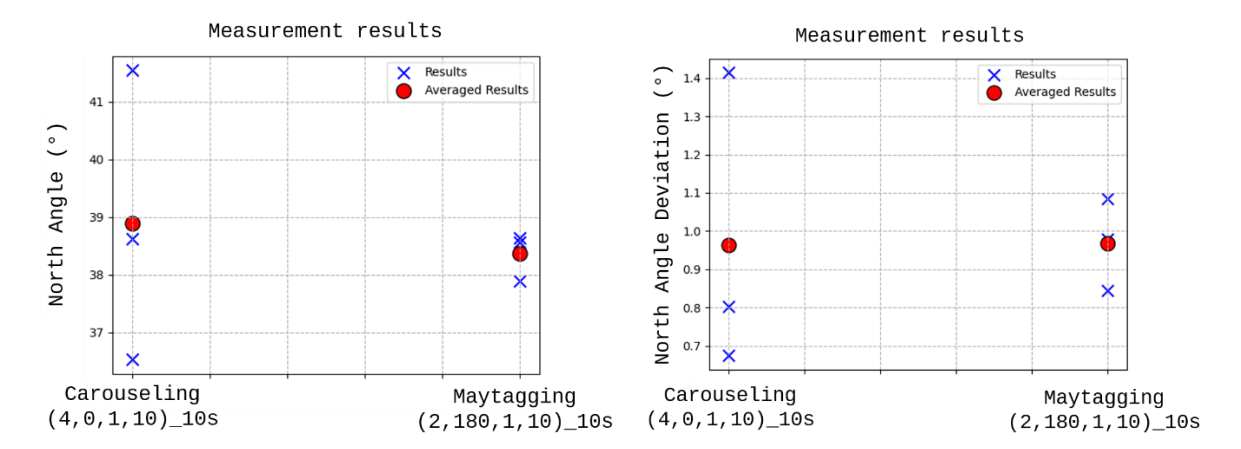


Figure 29: Measurements results of North Finding experience of a Carouseling and a Maytagging.

This difference can be explained by the nature of the Maytagging method compared to Carouseling. Maytagging involves performing a measurement and then immediately its opposite at 180°, which allows for the direct subtraction of biases and systematic errors. As a result, for an equivalent total signal acquisition time, Maytagging appears to provide greater accuracy. However, it is important to note that due to these repeated 180° round trips, the Maytagging method requires more time to complete a full measurement cycle compared to Carouseling.

In addition, the observed differences in standard deviation between the measurements and the simulation results can be explained by the difference in signal complexity. As illustrated in Figure 20, the FFT of the simulated signal successfully replicates the general shape of the measured signal. However, the simulation does not include all real-world noise sources present during the measurements. This absence of additional noise in the simulation environment results in lower variability and artificially higher precision compared to the actual measurements.

Therefore, to conclude, by faithfully reproducing the key characteristics of the gyroscope's Allan variance and introducing a realistic noise environment, the simulator made it possible to compare various North Finding strategies, such as Carouseling and Maytagging, both in terms of accuracy and robustness. The simulation results, corroborated by experimental measurements, highlighted the superior consistency of the Maytagging method, thanks to its bias-cancellation mechanism. However, the goal of this simulator was to find a configuration that would allow a better accuracy in the results, which was not obvious. So instead, a visual difference in the configuration during the experiment has been searched.

7. North Finding Experiment

To implement the Carouseling and Maytagging methods of the North Finding experiment, I needed measuring instruments, rotating devices and an automatized script that would correctly do the measurements, which are:

a. Measuring instruments: MFLI & HF2LI

Two digital synchronous sensing instruments developed by Zurich Instruments were used for the gyroscope measurements: the MFLI and the HF2LI. These devices are highly accurate and stable. Thanks to LabOne, the user interface, both instruments offer an experience with advanced visualization and analysis tools integrated into a web browser page.

The MFLI



This MFLI is particularly suitable for measurements requiring high stability, low drift, and excellent time resolution. The MFLI is used for its measurement accuracy. It is used to send the excitation signal to the gyroscope and receives the Drive mode signal to operate the PLL and PID.

Figure 30: MFLI picture. (Instruments, MFLI Détection Synchrone, s.d.)

The HF2LI



Figure 31: HF2LI picture. (Instruments, HF2LI Détection Synchrone, s.d.)

The HF2LI is a little less accurate because it sweeps a wider frequency range than the MFLI while having the same analog-to-digital converter, which makes its elementary step larger and therefore less accurate for the control of the different electronic loops, used (PLL / PID). It receives the signal from Drive mode and Sense mode. The measurements are made on this device, because it has two inputs, while the MFLI has only one.

The selection of the measurement instruments is now complete, providing a foundation for the experimental setup. However, one essential component is still missing: the motor that will allow precise orientation of the gyroscope at different angles. The next section of this report will therefore focus on the implementation of this motorized positioning system.

b. VIXEN SPHINX Telescope Mount & Stepper & CAD Part

To the Earth's angular speed, the VIXEN Sphinx telescope mount was the first solution: its motors ensured precise movement, about an arc second, while its integrated software, STARBOOK, provided freedom of movement around the axis of the North Star to perform the various scenarios. (Vixen, s.d.)

The telescope mount is crucial for its angular precision, allowing for reliable measurements unaffected by the uncertainty introduced by the mount's motors. Designed for astronomy, this motorized mount offers high pointing accuracy, mechanical stability, making it an excellent positioning tool for this type of experiment. Since the experimental environment requires thermal equilibrium, the mount is controlled remotely using a Python library to program the various positions as the scenarios progress. The ASCOM software and the Alpaca library were key elements in this step. In fact, by using the ASCOM Remote server, it is possible to communicate via WEB API protocols with the software interface included in the mount to control the positions in which it must be placed. (Initiative, 1998)

Setting up and controlling the mount required a significant amount of time and experimentation. Initially unfamiliar with the device, I began by performing manual control using dedicated software on the computer to understand its basic functioning. The possibility of bypassing the STAR BOOK controller to directly control the mount's motors was explored, but the complexity of the mount's motor control system made this approach unfeasible with the time available.

Ultimately, a more reliable solution using the ASCOM software environment was selected. One of the major challenges was integrating the mount into the closed ONERA network. There were several unsuccessful attempts, due to the age of the mount and the high speed of the ONERA network, causing compatibility issues. After identifying and addressing these limitations, it was possible to establish a stable connection, allowing full remote control of the mount from a computer within the network.



Figure 32: Image of the telescope mount in use, left. Top right, a zoomed-in view of the gyroscope's grip area. Bottom right, an image of the STARBOOK in use with the mount.

However, there were mechanical constraints in the mount, which made it impossible to run a North Finding scenario correctly, so we had to integrate a new device: a stepper! The presence of the mount allows us to run the same scenario in different positions, which will potentially give us different information on the behaviour of the gyroscope.



Figure 33: Image of the SMC10 Stepper used during the experiment. (Newport, s.d.)

As the parts were not at all compatible with each other, it was necessary to make adaptation parts between the VIXEN mount, the stepper, and the gyroscope:

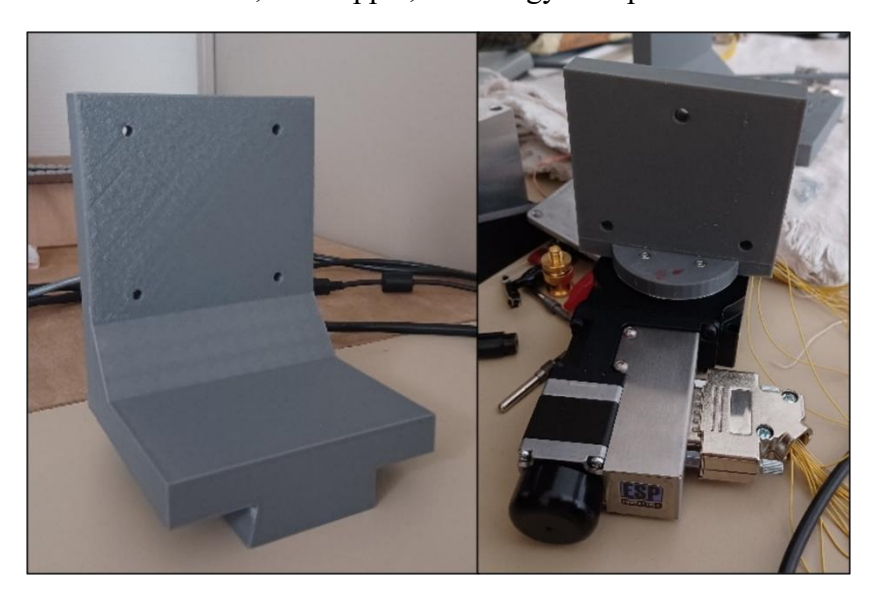


Figure 34: Image of CAD parts printed at the ONERA center at Palaiseau. I designed those two parts with a co-worker Ismaël, using his experience in SolidWorks.

Therefore, all the devices are now identified, but did not work together. The following step of the report is to connect all these devices together by creating a new Python script to control all those devices in one script.

c. Setting up the experiment with a Python script

To carry out the experiment, I need to connect all the devices together. The following figure shows the relationships between the different devices: the MFLI and the HF2LI are the measuring instruments of the gyroscope whose orientation depends on the stepper and the telescope mount. The computer controls the measuring instruments, the stepper and the mount. The gyroscope and the telescope mount are powered by a power supply because the gyroscope

needs a voltage of +/- 5V and a current of 100mA. The telescope mount needs a voltage of 12V and a current of 2.8A: figure 35.

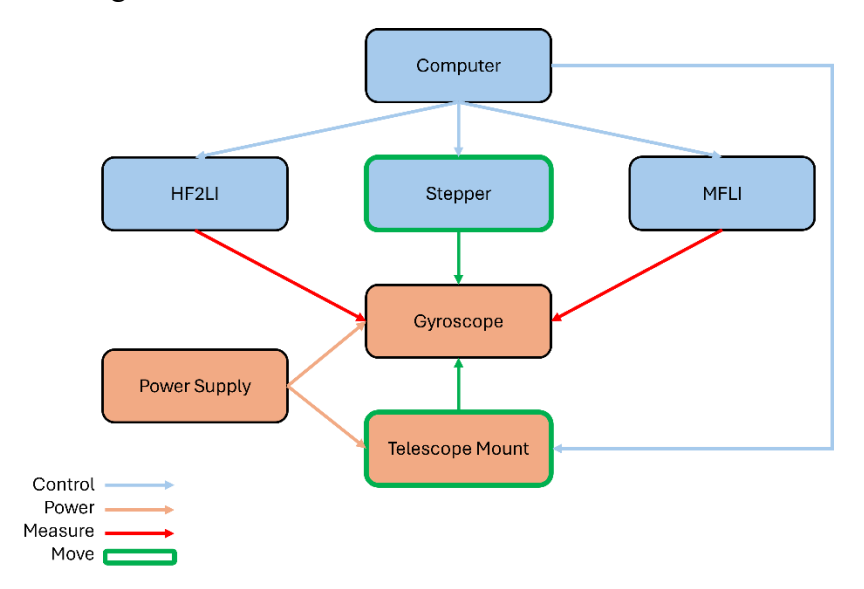


Figure 35: Diagram showing the relationships between the different devices used.

Figure 36 shows the general steps performed during a Northern Research experiment, including the use of the devices and characterization tools presented so far:

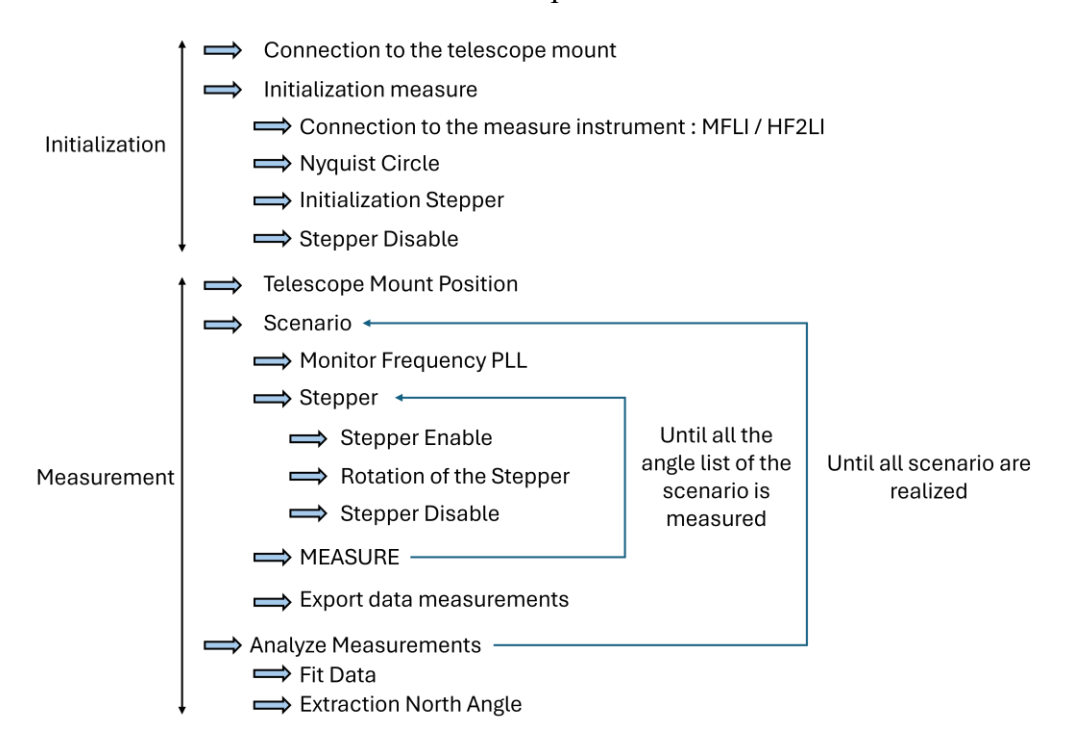


Figure 36: General steps of a North Finding experience.

The presentation of the devices used to set up the experiment is finished; the next part will focus on the results of the North Finding experiment done on a table to be sure the experiment was possible with the gyroscope.

d. First measurements...

Before making the full measurement with the telescope mount, measurements are first made on the table to verify that the gyroscope is indeed capable of measuring the Earth's rotation speed and to debug the code that sets up the whole experiment. Indeed, a single script controls the stepper that rotates the gyroscope, positions the telescope mount, controls the measuring devices, launches the measurements and finally, sorts the measured data to extract the sinusoid of the Earth's rotation speed and the North orientation!

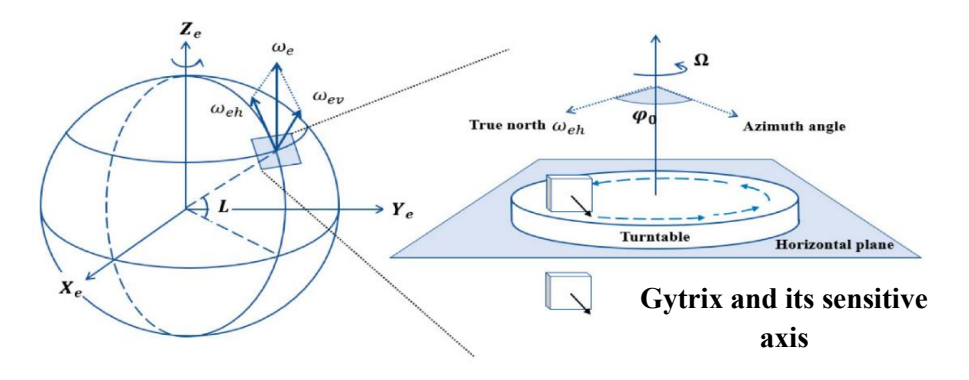


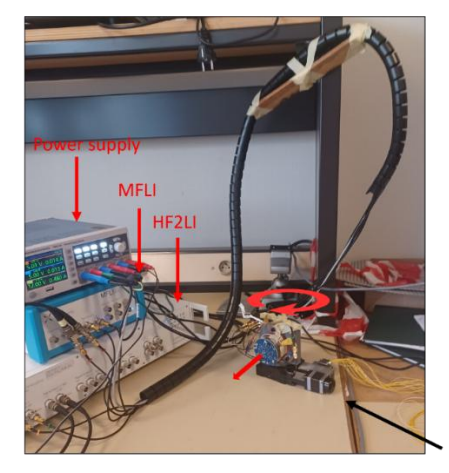
Figure 37: Schematic of a horizontal North Finding experiment. (Shuwei Fang, 2024)

The table measurement consists of using the stepper on top of a table to move the gyroscope in different orientations, as shown in the figure 37 on the right. This manipulation allows us to measure only the projection of the Earth's rotational speed horizontally, which corresponds to the quantity ω_{eh} in the figure 37 on the left. This positioning allows us to measure a signal of approximately 10°/h at the latitude of Châtillon (48°), instead of the 15°/h, which is the complete value of the rotational speed of the Earth, as seen in equation (12) and (13).

$$(12) \Omega_{Earth Rate} = \frac{360^{\circ}}{23h56 \min 4s} = 15.04^{\circ}/h$$

$$(13) \Omega_{projected Earth rate} = \Omega_{Earth Rate} * \cos(48) = 9.91^{\circ}/h$$

Therefore, the figure 38 is a picture of the initial setup on the table:



Stepper: Spins the gyrometer

Figure 38: First implementation of North Finding experiment.

The MFLI and HF2LI are connected as explained previously; the gyroscope is on the stepper. The figure 39 shows a measurement result made in this configuration:

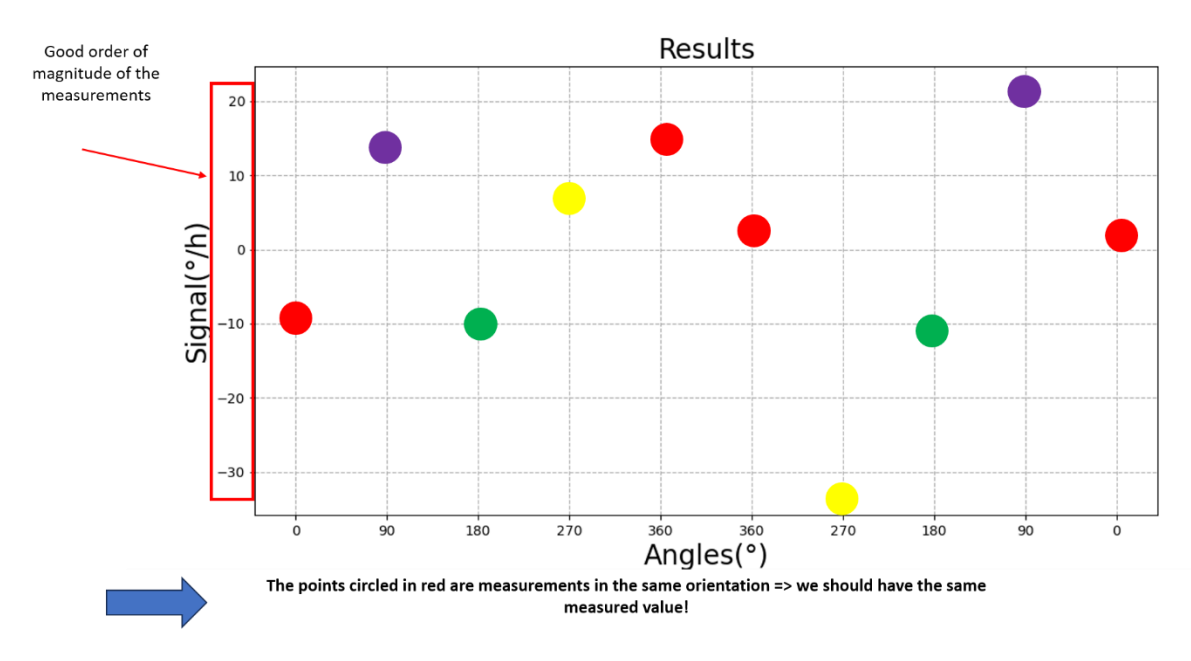


Figure 39: First measurements results of the North Finding experiment.

Even though, the results are in the right order of magnitude, the measurements are not consistent; the points surrounded by the same colour should be aligned. There could be a general trend due to a temperature drift, for example, but this is not the case, because it would affect all the points or, the trend of the purple points is positive while that of the yellow points is negative. The first measurements made in this configuration did not work at all. By analysing the environment of the experiment, we were able to deduce the potential causes of this first failure:

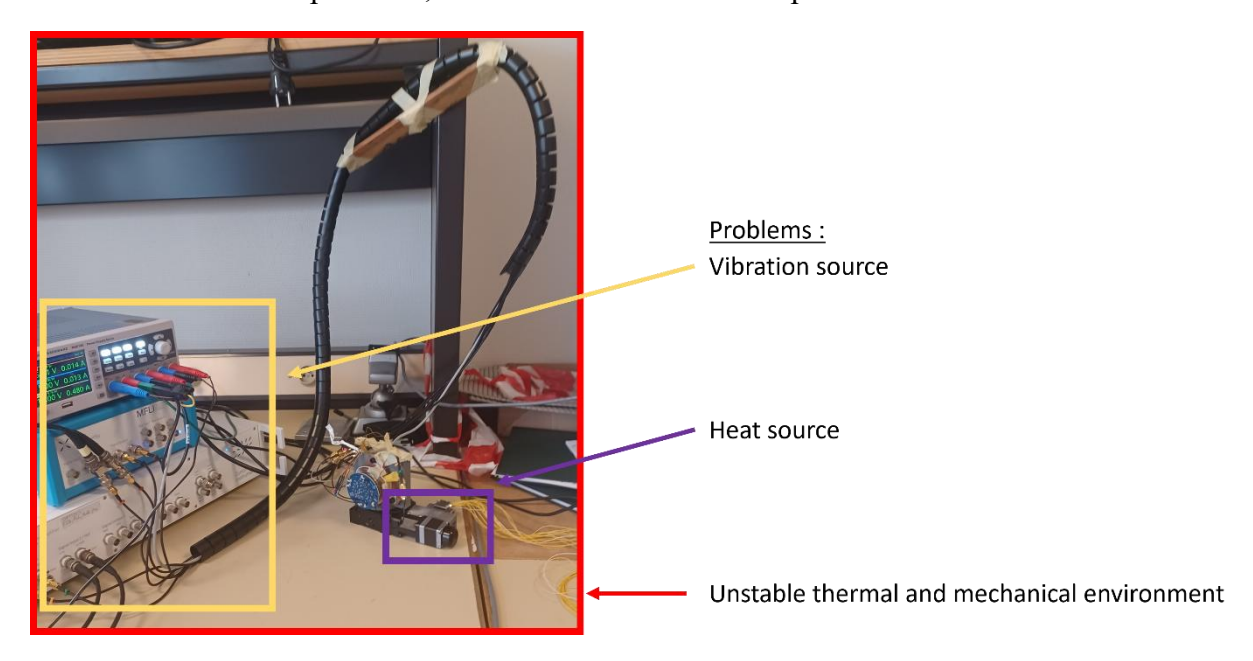


Figure 40: Image showing potential noise sources during measurement.

There were mechanical and thermal disturbances in the room: the instruments were placed next to the gyroscope on the same table and even if they did not seem to vibrate much, it can still have an impact on the measurement. The thermal environment is not very stable either; there are windows a meter away from the experiment. In addition to that, I realized that the stepper was heating up a lot at the motor level, which is aside to the gyroscope's rotation axis. Therefore, at each measurement, there were measurement points where the gyroscope was just above the heat source and others where it was not. This adds a big variation in temperature. To address these issues, the measurement setup was changed, and the measurement script was modified to always disable the stepper torque except when the stepper was needed to rotate the gyroscope. This modification prevents the stepper from heating up. The experiment was then moved alone onto a plate to isolate mechanical vibrations and into a furnace for thermal insulation. The measuring instruments are placed outside the plate, as in figure 41.

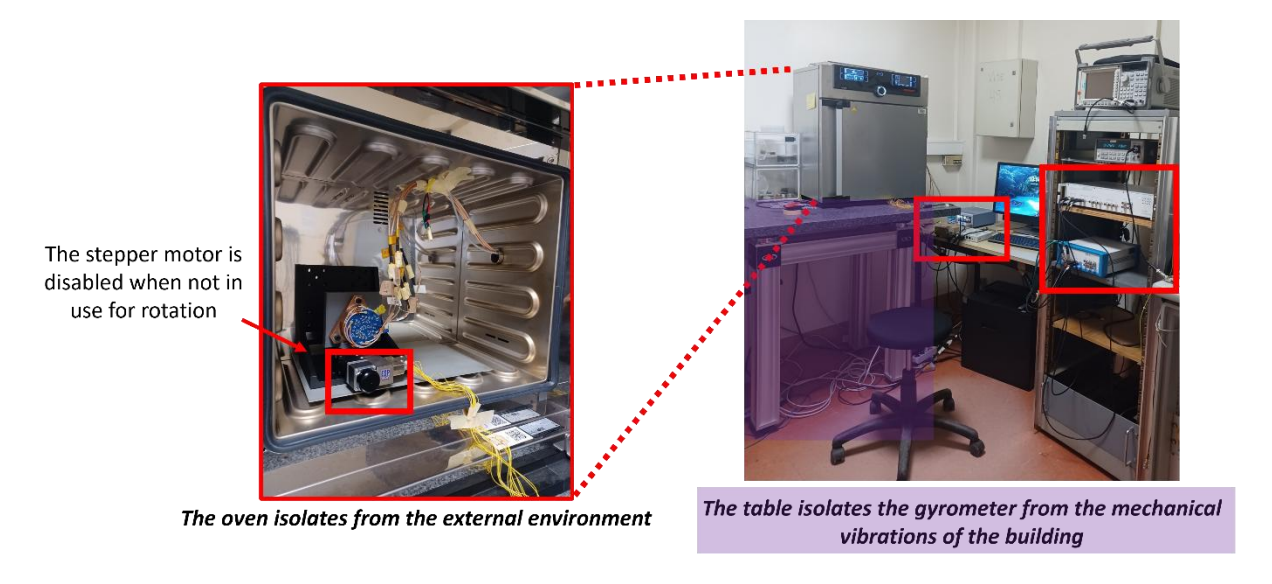


Figure 41: Second implementation of the North Finding experiment.

The first measurements work, the figure 42 represents the Maytagging measurements with a round trip and an increment of 1° between each measurement. Such a measurement takes several hours but we can see on the measurements that there is no general trend of the points, they remain stable over time.

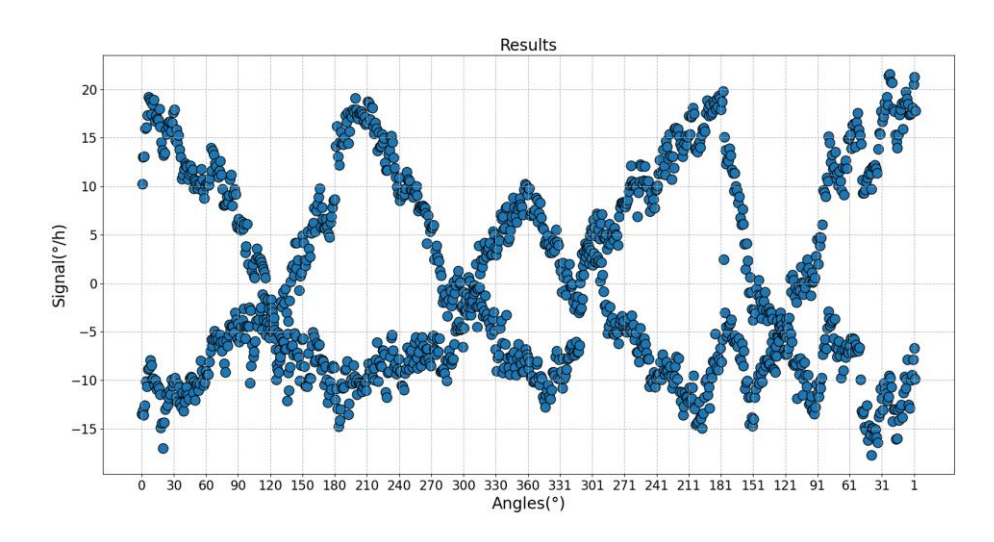


Figure 42: First functional results of North Finding. Measurement result. Scenario: Maytagging (2,180,1,1)_10s

We can observe that the figure 43 roughly follows the results of a sinusoid even if it is not perfect, there seems to be some disturbances in the measurements:

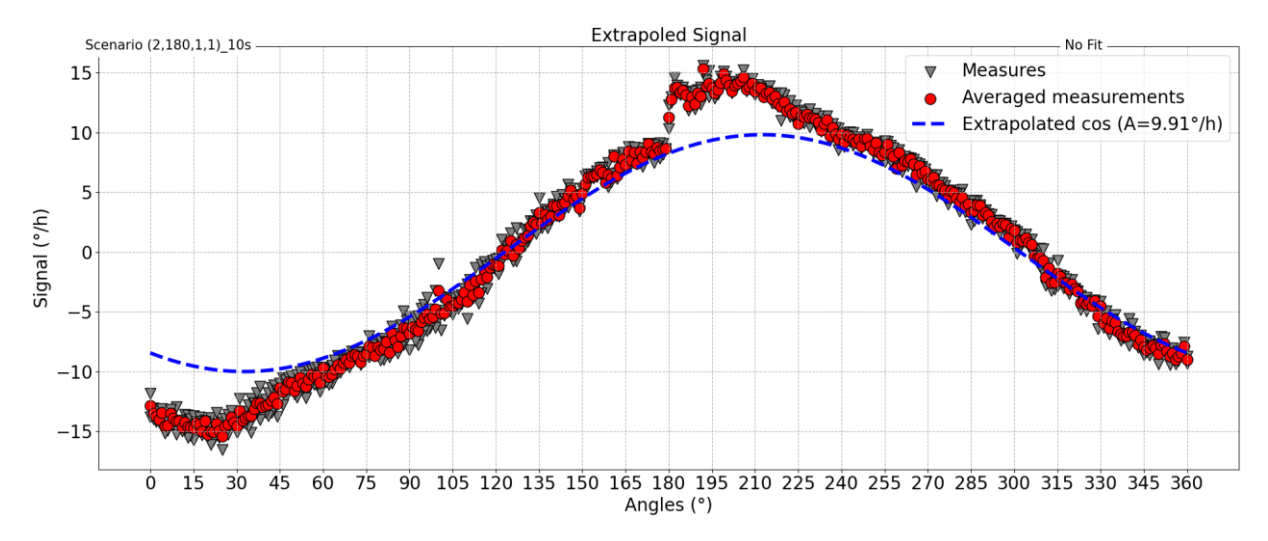


Figure 43: First functional results of North Finding Experiment. After analysing the results and extracting the North angle.

However, quickly the problems return because the series of measurements carried out the next day does not give the expected results; here is an example in figure 44:

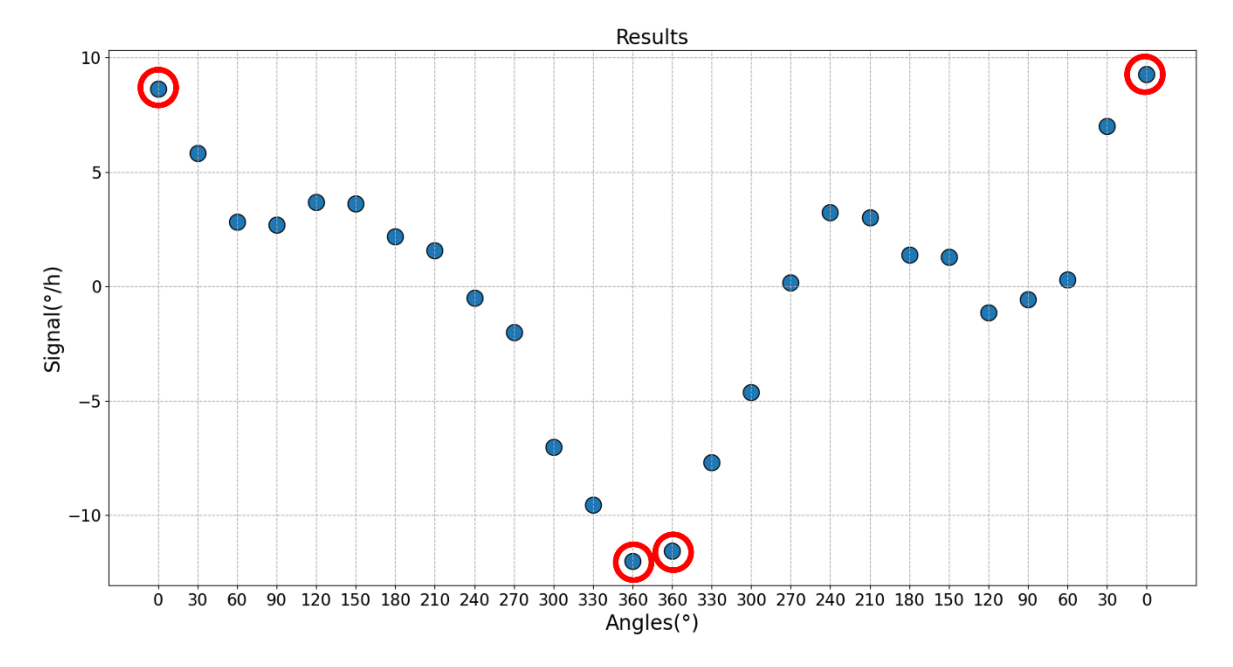


Figure 44: Measurement result failed. Scenario: Carouseling (2,0,1,30) 10s.

This figure 44 represents a round-trip Carouseling with a 30° increment between each measurement. Even though the measurement is not conclusive, we can still see a symmetry of the points in the results between the forward and backward ways except for the points circled in red. Indeed, the points circled in red are supposed to have the same value because they were measured at the same orientation. However, this is not the case, which means that there is a difference in the environment. By analysing the setup in the oven and looking at the difference between the 0° position and the 360° position (with an additional cable twist), it was noticed that in the 0° position, the cables that were hanging in front of the gyroscope, seemed to have

an influence on the measurements. A copper shield was added to avoid interference from the cables on the gyroscope, as showed in figure 45.

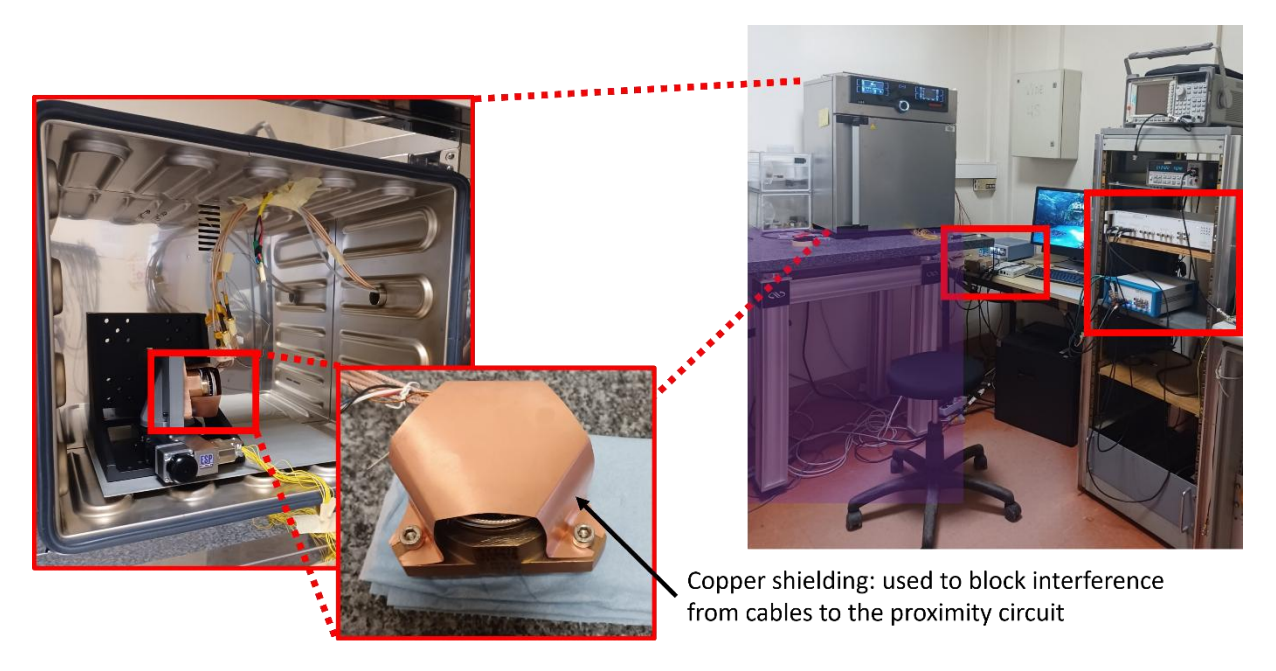


Figure 45: Improved setup of the North Finding experiment: addition of a copper shield.

The figures 46,47,48 and 49 show two results from Carouseling and Maytagging. These two scenarios were run to differentiate the two methods. Carouseling consists of two round trips with a 10° increment between each measurement, which lasts 10 seconds. Maytagging, having twice as many points, has only one round trip for the same scenario. Thus, these two scenarios have the same overall acquisition time and the same unit measurement time.

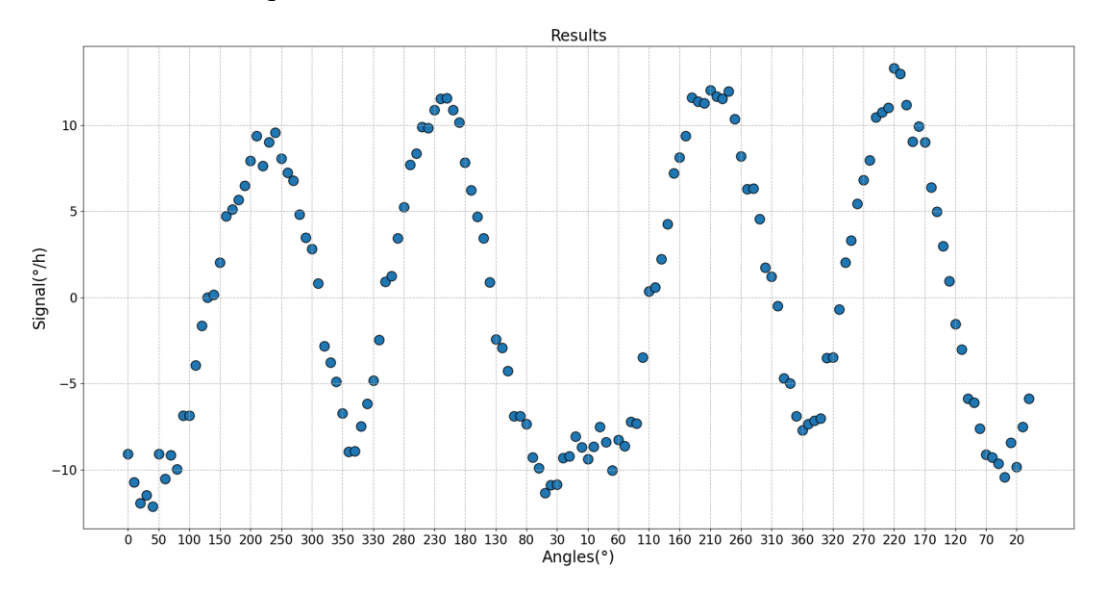


Figure 46: Carouseling measurement result. Scenario: (4, 0, 1, 10)_10s.

We can see that there is a slight thermal trend (increasing) present during the experiment. There is some noise in the measurements, but the shape of the sinusoid remains distinct. Analysing these measurements gives the following result:

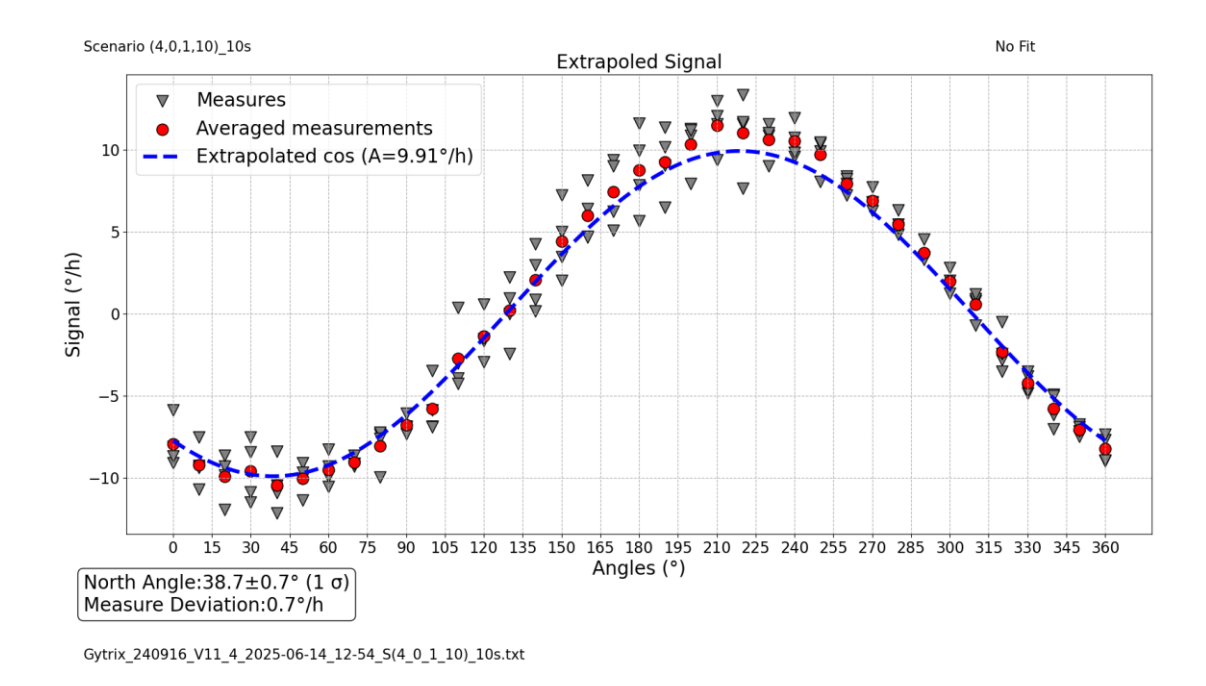


Figure 47: Analysis of Carouseling measurements and extraction of the North orientation relative to the local reference point. Scenario: (4, 0, 1, 10)_10s.

The Maytagging measurement, in figure 48, gives the following results, just as during the Carouseling measurement, there is a thermal trend that is present during the measurement but the advantage of Maytagging is that with the subtraction of two consecutive measurements, the biases cancel each other out. We can see from the analysis of the results in figure 48 that the points are much closer together between two same measurements while the thermal trend is stronger during the Maytagging measurement than that of the Carouseling.

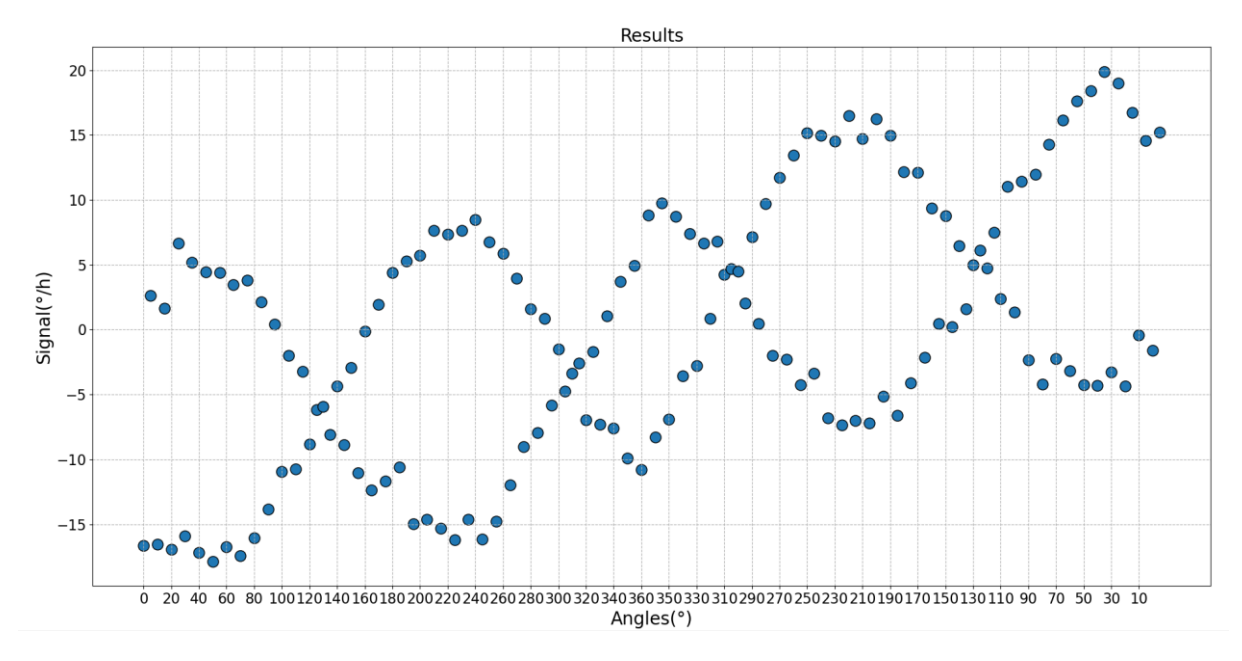


Figure 48: Maytagging measurement result. Scenario: (2, 180, 1, 10) 10s.

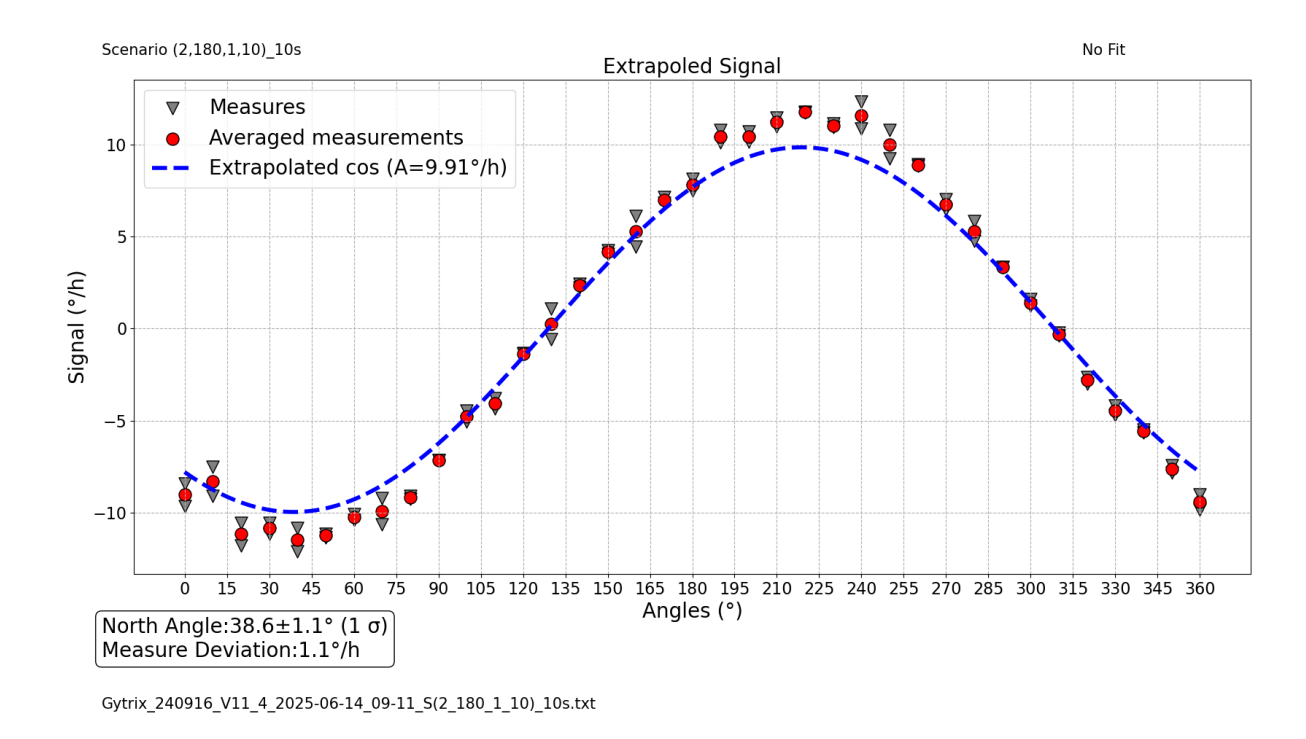


Figure 49: Analysis of Maytagging measurements and extraction of the North orientation relative to the local reference point. Scenario: (2,180, 1, 10) 10s.

Therefore, to compare the results of the North angle extraction, I estimated the North orientation to be about 38° give or take a few degrees. In fact, the building is oriented 38° from North and the furnace is aligned with the wall of the room in the building. Moreover, the gyroscope in the furnace has its starting point parallel to the back wall of the furnace.

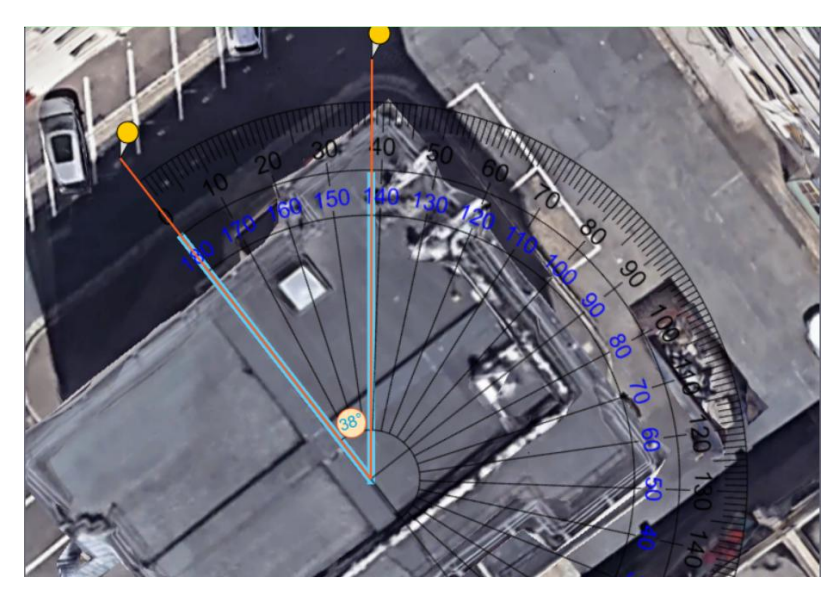


Figure 50: Orientation of the building relative to the North.

With this Carouseling, we find a North angle of 38.7° +/- 0.7°, while with Maytagging, the North angle is 38.6° +/- 1.1°. For this measurement, Carouseling appears to be more accurate than Maytagging. Accuracy still varies during the measurement, as biases varies. If the signal varies due to strong biases, it leads to greater uncertainties. In cases where biases are truly excessive, the script allows for bias correction by removing the trend on the points to straighten

them out. Similarly, in cases of a one-time event that results in a measurement with an aberrant result, there is an option in the script to remove certain aberrant points based on a distance criterion from the median of the points.

Moreover, Carouseling is also generally faster for the same number of measured points because the stepper does not make 180° rotations.

As a conclusion, this first setup allows us to measure the Earth's rotation speed and to extract a North orientation relative to the local reference point of the gyroscope. I was able to test the two North Finding methods: Maytagging and Carouseling and obtain satisfactory results for both. The next objective is to create a data simulator that will allow us to find the most accurate measurement configuration by simulations, without realizing any measurements. This will allow us to be able to find directly the most suited configurations depending on the gyroscope characteristics.

8. Complete North Finding Experiment with the Telescope Mount

The North Finding experiment in the oven has been a success, so the next goal is to use the telescope mount to tilt the gyroscope other than horizontally. It will allow us to learn more about the behaviour of the gyroscope. Indeed, the telescope mount can allow us to tilt the gyroscope to follow several paths, in figure 51.

<u>1 (No gravity)</u>: The first plane is horizontal: This situation is the same as the one with the gyroscope in the oven. In this case, we do not measure the entire component of the Earth, but only its projection onto the ground: that is $\Omega_E * \cos(\varphi)$, with φ being the latitude. This position also allows us to have an equal projection of gravity in all positions, and to avoid additional bias, at the expense of the signal to be measured, which is smaller (~ 10°/h instead of 15°/h if we measure the total component of the Earth's rotational velocity). Measuring again in this position will allow us to check that everything is correct and functioning well in this situation and compare the results with the ones that were made in the oven.

2&3 (Full rotation & Full gravity)&&(Full rotation & Partial gravity): The following two planes allow us to measure the entire component of the Earth's rotational velocity by passing through two different paths. The difference between these two paths is the projection of gravity, which is not the same; in one case, it is fully projected, and in the other, only partially.

4 (No rotation): The last plane is the one that allows us to measure zero rotational velocity throughout the entire measurement, keeping the sensitive axis always perpendicular to the Earth's rotational axis. This plane will allow us to verify whether the gyroscope is sensitive to anything other than the Earth's rotational velocity, such as gravity or the magnetic field, for example.

The figure 51 summarizes the four different planes that will be evaluated with the telescope mount.

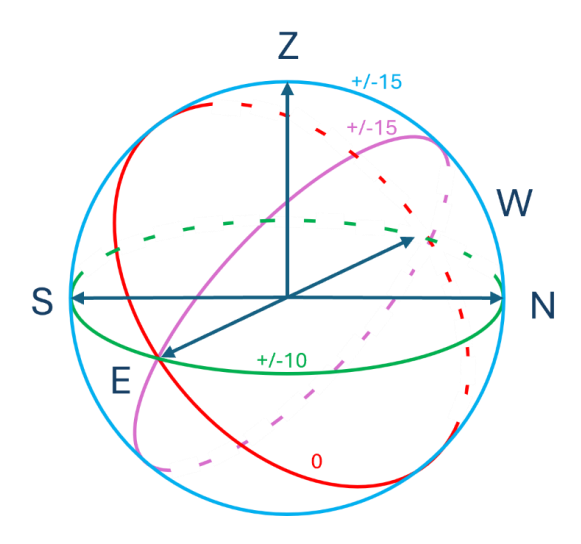


Figure 51: Graph representing the different rotation planes described.

To use the telescope mount, it needs to be aligned to the North Star. To do this, it was necessary to identify the orientation of the building with respect to the North and then transfer this angle to one of the walls of the building in the room where the measurement will be realized, to orient the mount.

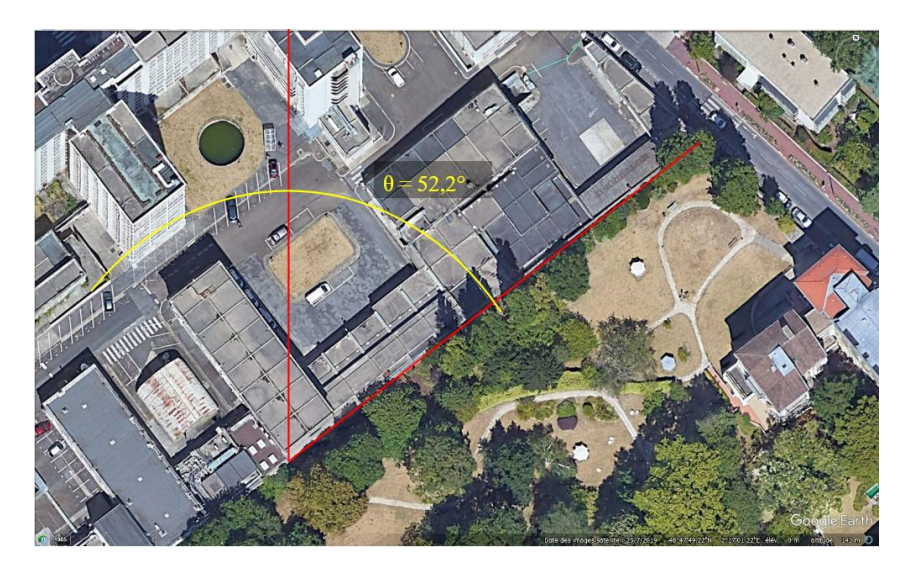


Figure 52: Orientation of the building with the geographic North, using a screenshot of Google Maps.

The North Finding experiment with the telescope mount is realized on the -2 floor to have a stable thermal environment and the minimum possible variation.



Figure 53: North-Finding experiment set up in the basement of an ONERA building. On the left, a complete view of the experiment. On the right, a zoom on the telescope mount with the construction lines on the ground to orient the mount relative to geographic North.

However, this experiment could not be launched at the writing time of this report because the gyroscope was behaving abnormally, preventing any accurate measurements. The cause of the error is being investigated, and the experiment will be launched later if time permits.

Conclusion

As a conclusion, during my PFE, I set up a North Finding experiment. Thanks to this project, I was able to work on the GYTRIX gyroscope developed by the CMT team. I learned the physics behind the functioning of this sensor through experimentation. I was able to set up the North Finding experiment with satisfactory results, estimating the orientation of North with about 1° accuracy. In addition, I set up a data simulator that allows simulating an output signal from the instrument based on the characteristics of the Allan variance. This simulator provided results that could be compared with the results of the instrument and showed satisfactory results. The North Finding experiment could have been pushed further by using the telescope mount, but a malfunction of the gyroscope prevented this implementation.

This work during this PFE opens up several approaches for improvement. The North Finding experiment can be launched when there is a sufficiently accurate gyroscope available, to explore the operation of the GYTRIX gyroscope. It will be possible to see if the gyroscope is sensitive to anything other than the angular speed, for example any magnetic field or gravity. It could be interesting to make a comparison between different gyroscopes to check the evolution of the results and see if there are representative of the reality. Finally, yet importantly implementation would be to find a way to shorten the North Finding Experiment to be able to only one or two measures like in the most advanced experiments and be able to find the North accurately with only two opposite measurements to remove bias. However, before doing those measurements, the GYTRIX needs to become more accurate.

Bibliography

- Asif, G. A. (2024). True north measurement: A comprehensive review of Carouseling and Maytagging methods of gyrocompassing. *Elsevier Measurement*, p. 16.
- David C. RIFE, R. R. (1974, September 5). Single-Tone Parameter Estimation from Discrete-Time Observations. *IEEE TRANSACTIONS ON INFORMATION THEORY*, p. 8.
- DELAHAYE, L. (2021). *Vibrating inertial sensors : digital architecture and calibration.* Châtillon.
- Initiative, T. A. (1998). *Universal Standards for Astronomy*. Retrieved from ASCOM Standard: https://ascom-standards.org/
- Instruments, Z. (n.d.). *HF2LI Détection Synchrone*. Retrieved from Zurich Instruments: https://www.zhinst.com/europe/fr/products/hf2li-lock-in-amplifier
- Instruments, Z. (n.d.). *MFLI Détection Synchrone*. Retrieved from Zurich Instruments: https://www.zhinst.com/europe/fr/products/mfli-lock-in-amplifier
- Lucian Ioan Iozan, M. K.-J. (2010). North Finding System Using a MEMS Gyroscope. p. 8.
- Missions et Objectifs. (n.d.). Retrieved from L'ONERA: https://www.onera.fr/fr/missions-et-objectifs
- Newport, M. (n.d.). *SMC100 Single-Axis DC or Stepper Motion Controller*. Retrieved from https://www.newport.com/f/smc100-single-axis-dc-or-stepper-motion-controller
- Sagnac Effect. (n.d.). Retrieved from https://en.wikipedia.org/wiki/Sagnac effect
- Shuwei Fang, S. M. (2024). A Segmented Cross-Correlation Algorithm for Dynamic North Finding Using Fiber Optic Gyroscopes. *Sensors*.
- Thomas Perrier, O. L. (2022). Gytrix, a novel axisymmetric quartz MEMS gyrometer for navigation purpose. *IEEE International Symposium on Inertial Sensors and Systems (INERTIAL)*, p. 4.
- Vixen. (n.d.). *Vexen Telescope Mount*. Retrieved from Vixen | Producer of optics from astronomical telescopes and binoculars: https://global.vixen.co.jp/en/product/25049_3/

Annexes

Annexe A: Gantt chart

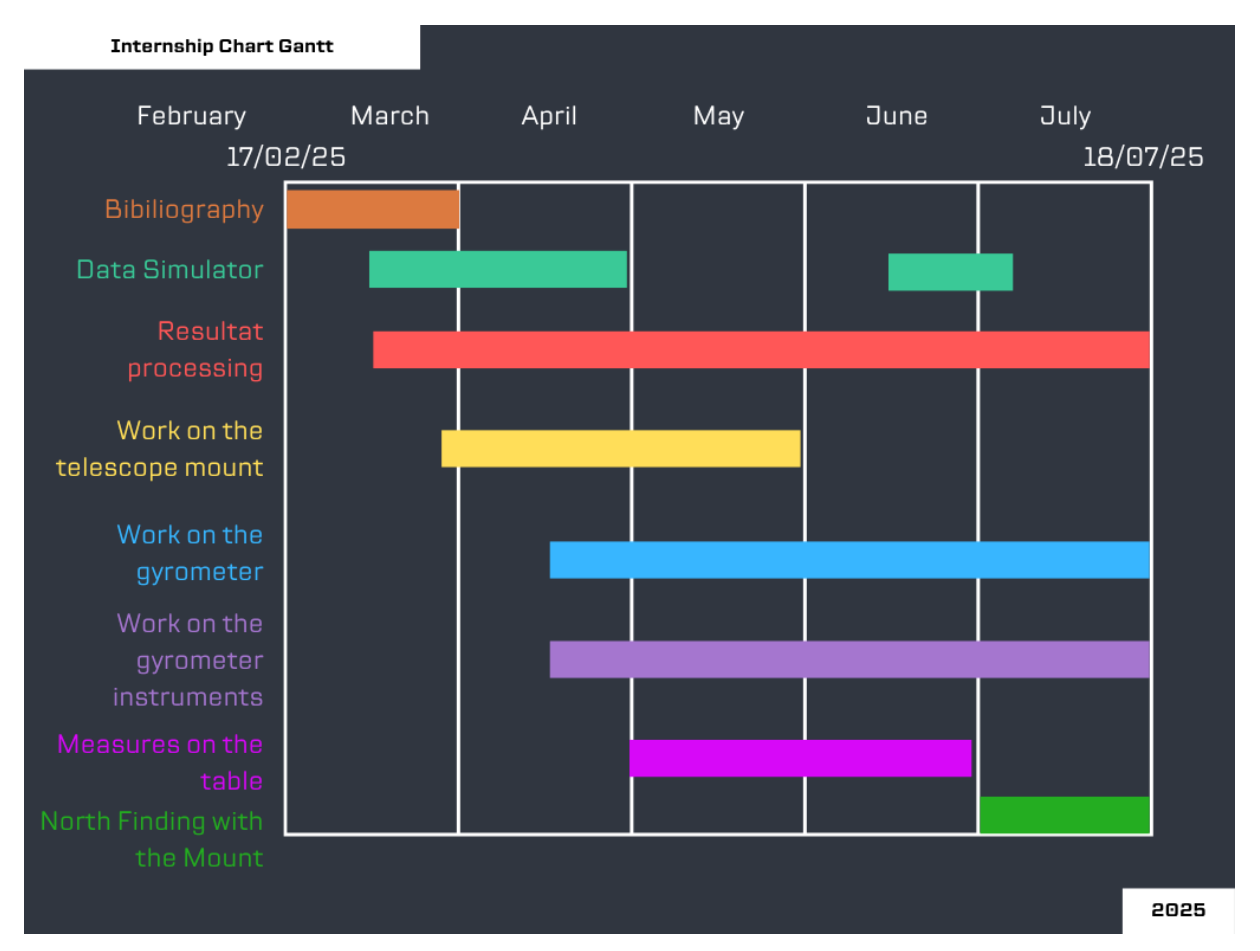


Figure 54: Gantt chart.

This Gantt chart shows the breakdown of the various tasks carried out during my internship, which took place from February 17 to July 18, 2025. It shows the main stages of the project: bibliographic research, development of simulation tools, processing of results, as well as experimental work on the telescope mount and the gyroscope. The schedule highlights the overlapping phases and the progressive evolution of the project, ranging from theoretical preparation to experimental tests and experiment.

Annexe B: Data Processing

This part of the code is dedicated to data processing; the same code is used whether the results are simulations or experimental measurements.

The goal of this script to process the data is to extract a value for the angle between geographic North and the local coordinate system. The first step is to sort the measurements in the correct order. Indeed, there may be multiple repetitions following the same measurement, or it may be a case of Maytagging. The details of the code are provided in the appendix, but to summarize the code's work, knowing the structure of the scenario used, rearranges the points in the correct order. The first step of data processing:

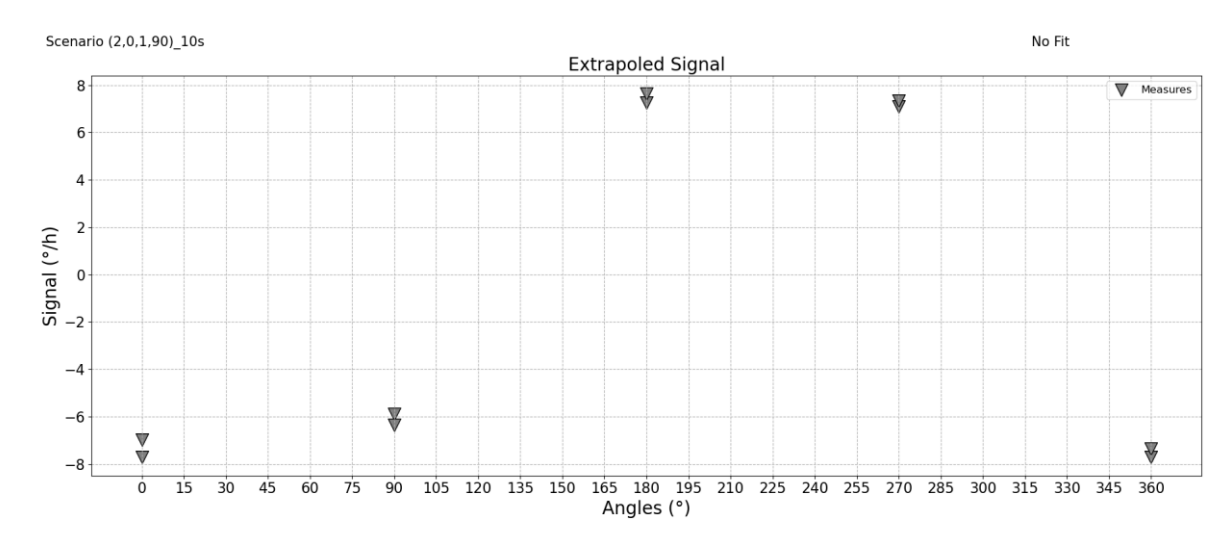


Figure 55: Display of averaged measurements of the Earth's rotation speed sorted by measurement orientation angle.

The next step is to average all points corresponding to a measurement at the same orientation:

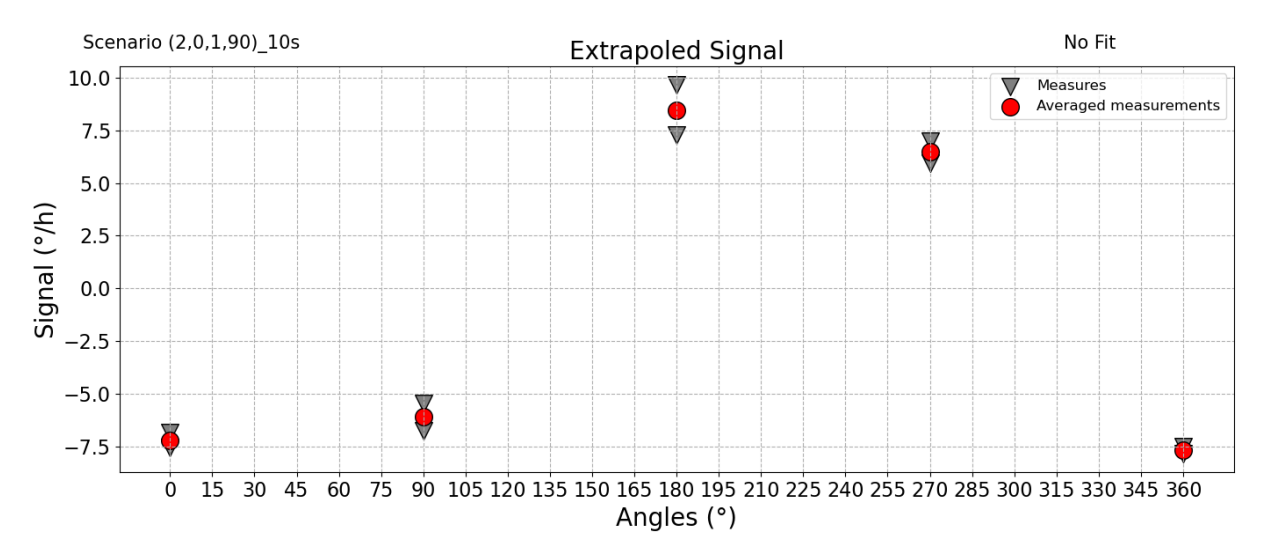


Figure 56: Averaging measurements sorted by angle value.

And finally, we need to extract the North angle from these points. To do this, we use a cosine fit with the averaged points, which are shown in red in the previous figure. We use the least squares method and a cosine of this form:

$$A * \cos(\Psi + \theta) + C$$

Where A represents the amplitude of the cosine, Ψ the orientation of the gyroscope in the local reference frame, θ the orientation of North relative to the local reference frame and C a bias in the measurements. The amplitude of the cosine is set to an expected value, 15°/h if we measure the rotation speed of the Earth while being in the axis of rotation of the Earth or another value which corresponds to the projection of the rotation speed of the Earth on the ground, depending on the latitude. In the case of this simulation, the simulation is done in the case where we are flat on the ground at the latitude of Chatillon, i.e. $48^{\circ}48^{\circ}$, which corresponds to an amplitude of the Earth rotation speed signal of $9.91^{\circ}/h$. By extracting the phase of the cosine, we obtain a value of the angle between North and the local reference frame of the gyroscope:

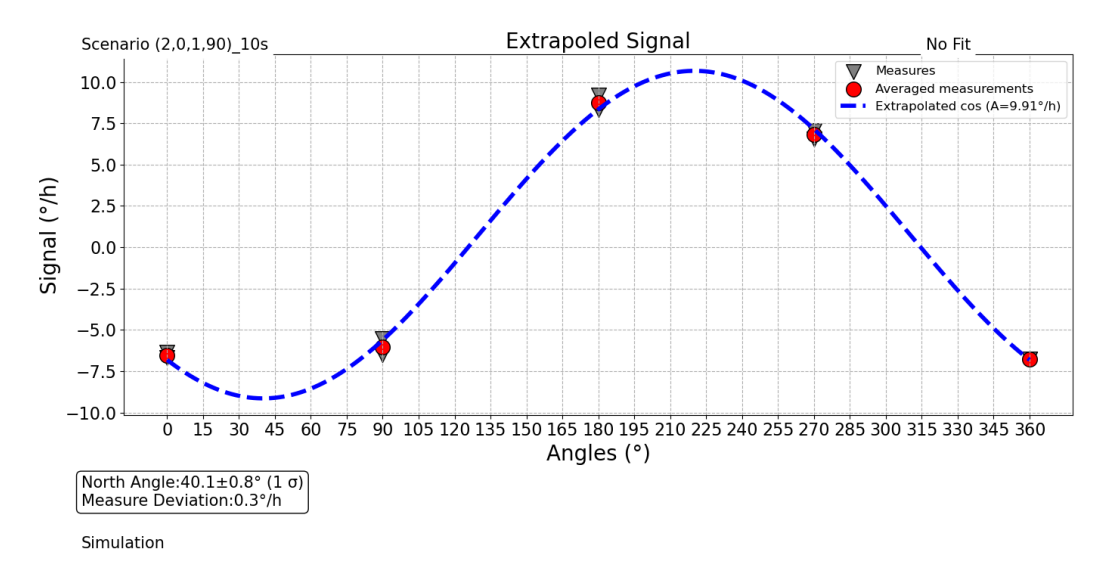


Figure 57: Extraction of a cosine of amplitude 9.91°/h whose phase corresponds to the orientation of the local reference point relative to the North.

To obtain a precise value for the North angle, I use the formula extracted from a scientific article (David C. RIFE, 1974) which allows to obtain a standard deviation value of a sinusoid knowing the frequency of the points and the amplitude, which is our case!

Before using the formula, it is necessary to obtain a precision on the measurements made: it is enough to calculate the variance between the measured/simulated points with respect to the expected sinusoid. We obtain σ_M .

By applying the formula, with A the amplitude of the expected sinusoid, N the number of measurements and σ_M the standard deviation on the measurement, we obtain σ_θ , the standard deviation on the angle:

$$\sigma_{ heta} = \sqrt{rac{\sigma_{M}^{2}}{A^{2}*N}}*rac{180}{\pi}degr$$
és $\sigma_{ heta} = 0.8\,^{\circ}$

So, an example of a result obtained with the data simulator is: $40.1\pm0.8^{\circ}$

So, for the moment, I have implemented two Python scripts that allow us to generate signals using the actual characteristics of the gyroscope to simulate North Finding experiments. The other part of the code allows us to sort the measured or simulated data to extract the information we are interested in: A measurement of the North orientation and its accuracy. The next step with this simulator is to make simulations to perhaps find an optimal scenario for this gyroscope.

Annexe C: Scenario Description

This part explains the five numbers used to describe a Maytagging or a Carouseling measurement.

A scenario is defined as a Maytagging or Carouseling measurement, and a measurement is defined as a measurement taken during the execution of a Maytagging or Carouseling procedure, for example, a 30° orientation measurement.

To simplify understanding and visualize more quickly, a form has been created to describe both methods.

It is broken down into five figures:

- N_{turn} : This represents the total number of turns performed during the scenario.
- A_{inv} : This indicates whether the scenario is a Carouse or a Maytagging scenario. In the case of Maytagging, $A_{inv}=180$ represents the 180° inversion performed at each measure, and for Carouseling, $A_{inv}=0$, which does not perform an inversion after each measure.
- N_{repet} : This represents the number of repetitions of a single measure in the case of Carouseling, or two measures in the case of Maytagging. For example, for Carouseling where N_{repet} =1, the list of angles where the measurement will be performed is 0°, 30°, 60°, ..., 300°, 330°, 360°. But in the case of the same Carouseling, where this time N_{repet} =2, the list of angles becomes: 0°, 0°, 30°, 30°, 60°, 60°, ..., 300°, 300°, 330°, 360°, 360°.
- A_{inc} : This represents the angle jumps between each measurement. It takes all values between [1°, 90°]. Having an increment beyond 90° means that the scenario will not take all four geographic orientations into account, which is not ideal when you want to orient yourself in space. In the example used in N_{repet} , A_{inc} =30.
- The fifth digit corresponds to the time of each measurement. This number is often determined by the shape of the gyroscope's Allan variance, as the chosen time corresponds to the minimum time at which the instability threshold is reached.

This form thus allows both methods to be represented in a single notation. It allows for a quick understanding of the scenario's form. For example, the scenario (2,0,1,10),10s is a Carouseling with a 10° increment, which performs one repetition for each measurement and two overall rotations.

Résumé

Dans le cadre de mon projet de fin d'études, j'ai développé et mis en œuvre une expérience de localisation du Nord géographique basée sur l'exploitation du gyromètre GYTRIX, capteur inertiel innovant concu par l'équipe CMT. L'objectif de ce travail est de réaliser une estimation précise de l'orientation du Nord par la mesure de la vitesse de rotation de la Terre, qui demande une précision de l'ordre du millième de degré-par-seconde au capteur. Cette étude m'a permis de renforcer mes compétences en physique des capteurs inertiels et en traitement du signal à travers des activités expérimentales et de modélisation. Afin de compléter les mesures expérimentales, un simulateur de données a été développé. Ce dernier génère des signaux synthétiques en reproduisant les caractéristiques statistiques du bruit du capteur, grâce à la prise en compte des caractéristiques de la variance d'Allan du gyromètre. Les comparaisons entre les données simulées et réelles ont montré la pertinence du modèle développé. Bien que certaines limitations techniques, liées à un dysfonctionnement du gyromètre, aient empêché la mise en œuvre finale de l'expérience sur monture équatoriale, les travaux réalisés constituent une base méthodologique et technique solide pour la poursuite du projet dès que le capteur sera à nouveau opérationnel. Les outils logiciels développés sont pleinement fonctionnels, commentés et prêts à être réutilisés dans le cadre de futures expérimentations.

<u>Mots-clés</u>: North Finding, gyromètre, GYTRIX, Simulation, Expérimentation, Instrumentation.

Abstract

As part of my end-of-studies project, I developed and implemented a geographic North-finding experiment based on the use of the GYTRIX gyroscope, an innovative inertial sensor designed by the CMT team. The objective of this work was to achieve a precise estimation of the North orientation by measuring the Earth's rotation rate, which requires the sensor to reach an accuracy about one thousandth of a degree per second. This study allowed me to strengthen my skills in inertial sensor physics and signal processing through both experimental work and modelling activities. To complement the experimental measurements, a data simulator was developed. This tool generates synthetic output signals by reproducing the statistical characteristics of the sensor noise, taking into account the specific Allan variance profile of the gyroscope. Comparisons between simulated and real data demonstrated the relevance and accuracy of the developed model. Although certain technical limitations, related to a malfunction of the gyroscope, prevented the final implementation of the experiment on an equatorial mount, the work carried out provides a solid methodological and technical foundation for the continuation of the project as soon as the sensor becomes operational again. The developed software tools are fully functional, documented, and ready to be reused for future experiments.

<u>Keywords</u>: North Finding, gyroscope, GYTRIX, Simulation, Experimentation, Instrumentation.

Sommario

Nel contesto del mio progetto di fine studi, ho sviluppato e realizzato un esperimento di localizzazione del Nord geografico basato sull'utilizzo del girometro GYTRIX, un sensore inerziale innovativo progettato dal team CMT. L'obiettivo di questo lavoro era ottenere una stima precisa dell'orientamento verso il Nord mediante la misurazione della velocità di rotazione terrestre, che richiede una precisione dell'ordine del millesimo di grado per secondo da parte del sensore. Questo studio mi ha permesso di approfondire le mie competenze nella fisica dei sensori inerziali e nell'elaborazione dei segnali, attraverso attività sia sperimentali che di modellizzazione. Per integrare le misure sperimentali, è stato sviluppato un simulatore di dati. Questo strumento genera segnali di uscita sintetici riproducendo le caratteristiche statistiche del rumore del sensore, tenendo conto in particolare del profilo della varianza di Allan del girometro. I confronti tra i dati simulati e quelli reali hanno evidenziato la validità e la coerenza del modello sviluppato. Sebbene alcune limitazioni tecniche, legate a un malfunzionamento del girometro, abbiano impedito la realizzazione finale dell'esperimento su una montatura equatoriale, il lavoro svolto costituisce una solida base metodologica e tecnica per la prosecuzione del progetto non appena il sensore tornerà operativo. Gli strumenti software sviluppati sono pienamente funzionali, documentati e pronti per essere riutilizzati in future sperimentazioni.

<u>Parole chiave</u>: North Finding, girometro, GYTRIX, simulazione, sperimentazione, strumentazione.

Summary Sheet

- 1. Student's identity: Camille Duclos
- 2. Phelma's engineering/Master program: Nanotech
- 3. Academic year: 2024/2025
- 4. *Title of the internship and period*: "Development and characterization of MEMS vibrating gyroscope electronics" from 17/02/2025 to 18/07/2025.
- 5. Logo, name, and postal address of the company/laboratory



ONERA

29 Av. de la Division Leclerc, 92320 Chatillon

- 6. First name, last name of the internship supervisor, and their email address: Jean GUERARD, jean.guerard@onera.fr
- 7. First name and last name of the school tutor: Liliana, PREJBEANU
- 8. The internship description initially validated by your Enterprise Relations Correspondent:

The vibrating accelerometers and gyroscopes developed at ONERA are miniature inertial sensors designed to achieve high performance in navigation or attitude control applications. They consist of a micro-machined quartz cell controlled by associated electronics. In the case of vibrating accelerometers, the resonance frequency of a vibrating plate connected to a test mass provides the acceleration. In the case of vibrating gyroscopes, the movement of a first resonance mode (the driver), combined with rotation, excites a second mode of the vibrating structure (the detector) via the Coriolis effect, the amplitude of which is then measured.

Specifically, a recent redesign of the gyrometric vibrating structure opens the way to a higher range of performance and, therefore, applications. However, this development requires a new architecture for the sensor and its electronics. The new cell, developed in the CMT research unit's microtechnology platform, enables operation in whole-angle gyroscopic mode, thanks to perfect symmetries between the pilot and detector resonances.

The intern will begin by studying the architectures of these inertial sensors and the associated electronic components: frequency synthesis, synchronous demodulation, PLL, and servocontrol. They will then take control of a measurement bench to characterize gyroscopes, working with control scripts (Python) and adapting scenarios. The intern will thus gain comprehensive experience in sensor development, from modelling the physical phenomenon to computer control of the instruments, to overall characterization of the instrument.

9. Resources (software, characterization equipment, office space, etc.) and supervision (technicians, assistant engineers, doctoral students, etc., in addition to the internship supervisor) provided by the company/laboratory.:

Software:

- Spyder (Python)
- LabOne (Zurich Instruments)
- ASCOM (Telescope Mount)
- Microsoft Package

Characterization equipment:

- Zurich Instrument: MFLI / HF2LI
- Multimeter
- Oscilloscope
- Binocular Microscope

Office Space:

- One desk to work on a fixed computer and screen.
- One laboratory desk to do experimentations with a fixed computer and a laboratory computer for the experiments.

Supervision:

- Two engineers who were also working with the instrument: from the fabrication to the characterization tests.
- The chef of the project who created the electronic board.